Micro-architecture of the human postnatal maxilla in relation to tooth development and eruption

By

Xolisiwe Mhlathi

(1502991)

Research dissertation

Submitted in fulfilment of the requirements for the degree

MSc in medicine

in

Anatomical Sciences

In the faculty of Health Sciences, University of the Witwatersrand, Johannesburg, South Africa

Supervisors:

Associate Professor Erin Hutchinson (BMedSci, BSc (Hons), MSc, PhD, PGDip (Edu))

Dr Candice Small (BSc, BSc (Hons), PhD)

11 February 2024

Declaration

I, Xolisiwe Mhlathi, declare that this is my own, unaided work. It is being submitted for a masters degree at the University of the Witwatersrand, Johannesburg. It has not been submitted before for any other degree or examination at any other university.

Xolisiwe Mhlathi Date: 01/12/2023

Abstract

The growth, modeling and remodeling of the maxilla are shaped by the biomechanical forces exerted on it. As functional demands of the masticatory system become more complex due to dental development and eruption, the intensity and complexity of the biomechanical forces increases and as such influences the associated bony micro-architecture. The knowledge gained from assessing the impact of these changes on the micro-architecture of the maxilla is important in the clinical and forensic contexts. Thus, this study aimed to assess changes in the micro-architecture of the alveolar region of postnatal and sub-adult human maxilla in relation to dental development and eruption. The study sample included seventy-nine individuals, subdivided into three groups according to dental development stages: deciduous dentition (n = 28; 0-5 years), mixed dentition (n = 9; 6-12 years), and permanent dentition (n = 42; 13-18 years). Maxillae were scanned using micro-computed tomography. Seven regions were selected along the buccal, lingual, and the apical surfaces of each dental crypt for evaluation of micro-architecture, which included bone volume fraction (BV/TV), trabecular thickness (TbTh), trabecular spacing (TbSp), material surface to material volume (BS/BV), and trabecular number (TbN). The micro-architecture of the maxilla changed from a more porous to a less porous nature, following patterns of bone remodeling during growth. These changes included an increase in BV/TV while BS/BV and TbN both significantly decreased. Thus, the trabeculae became more mineralized and decreased in number as they thickened. No significant differences were observed in TbTh and TbSp between the dentition groups. The observed micro-architecture reflects changes in the state of the dentition as well as adjustments to the complex functional environment of the oral cavity complex.

Key words: Maxilla, dentition, micro-architecture, Micro-CT, biomechanical forces

Acknowledgements

This project would not have been successful without the support from various people, and I would like to relay my gratitude to them. Firstly, I would like to thank my supervisors, Prof. Hutchinson and Dr Small, for designing this project and working with me to make it a success. They provided me with their expertise, advice, valuable comments, and overwhelming support throughout my masters journey. They did not only contribute to my growth as a researcher, but to my growth as a person as well. I am deeply indebted to them.

Secondly, I would like to thank the School of Anatomical Sciences for approving the study. My sincere gratitude goes out to the body donors, who, without them, this research would not be possible. And thank you to the board of the Raymond A. Dart Collection of Modern Human Skeletons for allowing the use of the material from the collection. I would also like to thank the South African Nuclear Energy corporation (NECSA) and Evolutionary Studies Institute (ESI) for allowing the use of their facilities for scanning and the analysis of the skulls, respectively.

A special thanks to my siblings, Zimasa, Sinekhaya, and Gcina for their steady love and support. They are the reason why I keep moving. I am also incredibly grateful to my friends, Thokozile Makhanya, Lutendo Mukwevho, Arthur Manjatika and Tabo Mwila, for their words of encouragement and support throughout this journey.

Lastly, I would like to thank the KIRSH foundation through the Wits Research Office and both my supervisors for funding this project.

Dedication

I dedicate this work to my brother, Makhosi, for all the support he has given me.

Presentations arising from this study

Mhlathi, X., Hutchinson, E.F. and Small, C. (2023). "Micro-architecture of the human postnatal maxilla across the stages of dentition". Oral presentation presented at the XXVIII International Symposium on Morphological Sciences conference. Cape Town, Western Cape, South Africa.

Table of Contents

List of figures

List of tables

List of abbreviations

ANOVA	Analysis of variance
AR	Apical region
BA	Buccal apical
BI	Buccal inferior
BM	Buccal middle
BS	Buccal Superior
BS/BV	Bone surface to bone volume ratio
BV/TV	Bone volume fraction
LA	Lingual apical
LI	Lingual inferior
LM	Lingual middle
LS	Lingual superior
Micro-CT	Micro computed tomography
NECSA	South African Nuclear Energy Corporation
ROI	Region of interest
SMI	Structure model index
TbTh	Trabecular thickness
TbN	Trabecular number
TbSp	Trabecular spacing
TEM	Technical error of measurement

1 Introduction

The masticatory system is a complex functional group of structures which include the mandible, maxilla, muscles of mastication, teeth, and the tongue (Buvinic *et al*., 2021). The growth, modeling and remodeling of both the maxilla and the mandible is shaped by biomechanical forces exerted on them (Akintoye, 2018). These biomechanical forces result from tooth development and eruption, muscle attachments and changes in the functional environment with growth such as the transition from suckling to mastication (Hutchinson *et al*., 2017; Akintoye, 2018; Buvinic *et al*., 2021). As the functional demands of the masticatory system become more complex due to the development and eruption of dentition, the intensity of biomechanical forces increases. These biomechanical forces affect bone micro-architecture by thickening the alveolar ridge and changing the trabecular morphology to a more compact structure (Lindh *et al*., 2004; Stauber and Müller, 2008; Kim *et al*., 2011; Blok *et al*., 2013; Kim and Henkin, 2015; Hutchinson *et al*., 2017). Knowledge gained from assessing and understanding the impact of these changes on the micro-architecture of the maxilla in relation to dental development and eruption is necessary for the planning of craniofacial surgical procedures by maxillofacial surgeons. In addition, knowledge of the development and growth patterns of the maxilla may assist osteologists in age estimations.

The maxilla forms by the process of intramembranous ossification, where mesenchymal tissue is directly converted to bone (Lee *et al*., 1992; Scheuer and Black, 2000). The ossification centers of the maxilla are observed around the sixth week of intrauterine life and are located above the dental lamina that gives rise to the developing dentition (Dixon, 1997; Scheuer and Black, 2000). In the eighth week of intrauterine life, the body of the maxilla and its four processes, which include the frontal, zygomatic, palatine, and alveolar processes, are identifiable. The alveolar process, which gives rise to dental crypts and will house the dentition, forms a bony gutter that envelopes the dental lamina. The dental crypts develop mesiodistally in the alveolar process and the inter-alveolar septa are the last parts to complete development in each dental crypt (Dixon, 1997; Scheuer and Black, 2000; Schaefer *et al*., 2009; Soriano and Das, 2022). The prenatal growth of the maxilla is influenced by the growth of associated structures, such as the appearance of the incisive fissure (Scheuer and Black, 2000). The incisive fissure is located on the oral surface of the palatine process and extends laterally and forward on both sides from the incisive foramen to the interval between the lateral incisor and the canine tooth (Trevizan *et al*., 2018) and plays a role in accommodating the increasing volume of tooth germs in the alveolar process (Scheuer and Black, 2000). In addition, the development of the maxillary sinus plays a major role in increasing the height of the maxilla (Dixon, 1997). While features such as the incisive fossa and maxillary sinus may play a role in the development of the face, it is important to have a sound understanding of how the underlying bony architecture changes in response to dental development, particularly when considering instances where the dentition may become impacted.

The developed maxilla is characterized by the basal and the alveolar bones, which are located on the superior and inferior aspects of the bone, respectively (Scheuer and Black, 2000; Park *et al*., 2008). The alveolar process consists of mainly trabecular bone covered by a thin layer of cortical bone and houses the dental crypts with the associated dentition. Each dental crypt spans from the apex (the floor) to the rim (the alveolar crest) of the alveolar process (Scheuer and Black, 2000; Gahleitner *et al*., 2003). The individual dental crypts are divided by inter-dental (interalveolar) septa. In multirooted teeth, there is space between the roots called interradicular septum (Scheuer and Black, 2000; Gahleitner *et al*., 2003; Kamigaki *et al*., 2017; Soriano and Das, 2022). Postnatally, the maxilla grows rapidly, and its growth is related to the functional areas of the viscerocranium, including the orbit and its contents as well as the nasal cavity and associated paranasal sinuses (Enlow and Bang, 1965; Scheuer and Black, 2000). The major influence of maxillary growth and changes in internal micro-architecture postnatally is the requirement for space to accommodate the increasing size and number of the teeth, which are associated with changes in functional environment such as the shift from suckling to mastication (Scheuer and Black, 2000; Buvinic *et al*., 2021).

In line with the maxilla, the development of the dentition begins at approximately six weeks of intrauterine life and continues until early adult hood (~ 18 years) (Scheuer and Black, 2000; Hovorakova *et al*., 2018). The deciduous dentition starts erupting at approximately six months postnatally (Scheuer and Black, 2000; AlQahtani *et al*., 2010). At approximately three years postnatally, all the deciduous teeth have erupted. The eruption of all the permanent teeth, with the exception of third molars, occurs between six and 12 years (Scheuer and Black, 2000; Liversidge, 2003; AlQahtani *et al*., 2010; Esan and Schepartz, 2018). This period is characterized by shedding of deciduous teeth and replacement by their permanent successors (AlQahtani *et al*., 2010; Esan and Schepartz, 2018). The last permanent tooth, the third molar, is not fully erupted until early adult life (Scheuer and Black, 2000). In some cases, the third molar does not develop at all (Sisman *et al*., 2007). In line with the staged development and eruption of the dentition, it is important to gain knowledge into the interplay between how the supporting bony architecture changes relative to the individual teeth as well as across various states of the dentition.

To facilitate the eruption of the dentition, the teeth must move through the alveolar bone (Nanci, 2007; Wise and King, 2008). The dental follicle and bone turnover form the basis of tooth eruption. The dental follicle intervenes between the alveolar bone and the tooth structure, and its role is to regulate the remodeling of the neighboring tissues. Bone turnover, which is regulated both temporarily and spatially, functions to facilitate the translocation of teeth in the alveolar bone (Kardos, 1996; Nanci, 2007; Wise and King, 2008; Maltha, 2014). The movement of teeth through the alveolar bone can be divided into three phases: preeruptive, eruptive and posteruptive tooth movements. The preeruptive movement occurs in both deciduous and permanent tooth germs within the alveolar bone before eruption begins. The eruptive movement of teeth occurs when teeth move from their position within the alveolar bone to their functional position in occlusion. Lastly, the posteruptive tooth movement is needed for maintaining the position of the erupted teeth in occlusion while the maxilla and the mandible continue to grow. It functions in compensating for the occlusal and proximal tooth wear (Nanci, 2007).

During the preeruptive tooth movement stage, the deciduous tooth germs are relatively small and there is a lot of space available in the jaw. However, these tooth germs grow very quickly and become crowded (Scheuer and Black, 2000; Nanci, 2007). The jaws lengthen to reduce the crowding, and this allows the deciduous molar tooth germs to move in a distal direction and the anterior tooth germs to gradually move in a mesial direction (Scheuer and Black, 2000; Nanci, 2007; Wise and King, 2008). As the jaws continue to increase in length, width, and height, the tooth germs continue to move outward and upwards within the alveolar bone (Nanci, 2007). The permanent tooth germs, which develop on the lingual side of their deciduous predecessors also move considerably within the alveolar bone as the jaws develop (Scheuer and Black, 2000; Nanci, 2007). The permanent anterior incisors and canines develop in their own crypts and move to the lingual side of the roots of the deciduous incisors and canines. Premolar tooth germs also move within the alveolar bone to be positioned between the roots of the deciduous molars (Scheuer and Black, 2000; Nanci, 2007; AlQahtani *et al.*, 2010; Esan and

Schepartz, 2018). Preeruptive movements of both the deciduous and the permanent tooth germs are said to be how the teeth are moved in position within the alveolar bone in preparation for the eruptive tooth movement (Nanci, 2007).

Eruptive tooth movement occurs when both deciduous and permanent teeth move from their developmental position within the alveolar bone to their final functional position in the occlusal plane (Nanci, 2007; Wise and King, 2008). Several mechanisms are required for the successful eruption of teeth including the remodeling of the alveolar bone and formation of the dental follicle and subsequently, the periodontal ligament (Kardos, 1996; Nanci, 2007; Wise and King, 2008; Maltha, 2014). While root formation may play some role in the eruption of teeth, it is not the cause, but rather a consequence of eruption. This relationship between tooth eruption and root formation is evidenced by the fact that teeth still erupt even in cases where root formation is incomplete or where teeth are missing roots (Nanci, 2007). As the teeth are encased within the alveolar bone, bone resorption is required for teeth to erupt. During bone resorption, which occurs on the occlusal surface of the maxillary bony crypts, teeth do not have to move for the eruption pathway to form (Nanci, 2007; Wise and King, 2008; Maltha, 2014). Follicular tissue is needed for these teeth to move within the alveolar bone and eventually erupt. Dental eruption is divided into two phases: the intraosseous phase and the supraosseous phase. During the intraosseous phase of eruption, the dental follicle is responsible for initiation and regulation of osteoclastogenesis and osteogenesis (Nanci, 2007). The dental follicle differentiates into the periodontal ligament and together with biomechanical forces, becomes responsible for moving the teeth into their functional occlusal position during the supra-osseous phase of eruption (Wise and King, 2008).

Posteruptive tooth movements occur after the teeth have reached their functional occlusal position and can be divided into three categories. These include the movements that occur to accommodate the growth of the maxilla and the mandible, movements that compensate for continuous occlusal wear, and finally, the movements that accommodate interproximal wear (Craddock and Youngson, 2004; Nanci, 2007). Movements for growth accommodation are seen as an adjustment of tooth socket position, which is achieved by new bone formation at both the alveolar crest and the tooth socket floor to match the increasing height of the jaws (Nanci, 2007). Compensation for occlusal wear is accomplished by continuous deposition of cementum around the apex of the tooth. Interproximal wear is compensated for by approximal drift, which is a process of tooth movement caused by, amongst other factors, occlusal force (Nanci, 2007)

The growth of the maxilla is not only related to the development and eruption of dentition, but also to the biomechanical forces exerted on it during mastication and swallowing (Thüer *et al*., 1999; Akintoye, 2018). The adaptation of the maxilla to biomechanical forces is not well understood due to its structural complexity (Peterson *et al*., 2006). The complexity of the maxilla results from the structures associated with it including the sutures and the paranasal sinuses (Scheuer and Black, 2000; Peterson *et al*., 2006). Maxillary morphology allows for a number of functions that are associated with development, including swallowing, the senses of smell and sight, respiration, as well as anchoring muscles of facial expression and a part of the masseter muscle (Enlow and Bang, 1965; Scheuer and Black, 2000; Peterson *et al*., 2006). When the biomechanical properties of the cortical bone of fresh-frozen adult dentate maxillae were investigated, it was found that the stress was greatest at the alveolar process and the body of the maxilla where biting force was exerted (Peterson *et al*., 2006).

Occlusal forces resulting from biting, mastication, and swallowing are exerted on the teeth and are transferred to the alveolar bone by the associated periodontal ligament (Van Eijden, 2000; Nanci, 2007; Yehuda *et al*., 2015). These forces are then converted into compression vectors around the root surfaces of the teeth and result in the remodeling of the alveolar bone in this region. The result of this remodeling is the trabeculae radiating from the roots and this arrangement helps limit the shear stress (Yehuda *et al*., 2015). The facial bones have a macro structure that is suited to enable maximal strength with minimal mass (Wolff 1986; Yehuda *et al*., 2015). In accordance with this principle, the loads on maxillary teeth will not only affect the alveolar bone, but also other associated structures like the orbits and the paranasal sinuses (Wolff, 1986). Overall, compression stress results in trabecular bone remodeling and torsion stress results in maintenance and remodeling of the cortical bone (Koch, 1917; Yehuda *et al*., 2015).

The proper alveolar process is only observed in the presence of teeth and is formed in response to dental development and eruption, indicating its close relationship with dentition. When the teeth are lost, the region is resorbed and becomes greatly reduced in height, with a sharp or round appearance (Ulm *et al*., 1999; Scheuer and Black, 2000; Roberts and Hartsfield, 2004; Farina *et al*., 2011; Kamigaki *et al*., 2017). Studies have reported on the metric and dimensional analysis of the maxillary alveolar bone (Farina *et al*., 2011; Pramstraller *et al*., 2011) Pramstraller *et al*. (2011) measured the ridge height and width of alveolar bone using micro-CT on a sample of 127 individuals with a mean age of 55.2±01 years. The results showed relatively low values in the alveolar bone height and width dimensions in edentulous maxillae when compared to dentulous maxillae (Pramstraller *et al*., 2011). Farina *et al*. (2011), using the same methodology, analyzed maxillary alveolar height of edentulous and dentulous sites in the distal regions of the same individual in a sample of 32 individuals. The results showed lower alveolar bone height measurements in edentulous sites when compared to dentulous sites (Farina *et al*., 2011). Similar studies also report the same trends of dimensional decrease in alveolar height and width in edentulous maxillae, emphasizing the influence of the dentition on the alveolar bone (Kopecka *et al*., 2012; Monje *et al*., 2013).

When assessing the trabecular micro-architecture of the alveolar process, some of the parameters that have been studied include connectivity density, structure model index (SMI) trabecular number, trabecular thickness, and trabecular spacing or separation (Parfitt, 1988; Stauber and Müller, 2008; Blok *et al*., 2013; Kim and Henkin, 2015). Connectivity density is the number of connections within the bone in a region of interest and indicates the mechanical strength of the trabecular micro-architecture (Parfitt, 1988; Stauber and Müller, 2008; Blok *et al*., 2013). The SMI is used to identify the difference between plate-like and rod-like trabecular micro-architecture. A lower SMI ratio indicates a more rod-like micro-architecture of trabeculae, which shows that there is more bone resorption (Kim and Henkin, 2015). Studies have looked at these features of the maxilla and mandible trabeculation in adult cadaveric and living individuals (Parfitt, 1988, Ulm *et al*., 1997; Stauber and Müller, 2008; Blok *et al*., 2013; Kim and Henkin, 2015). Monje *et al*. (2015) studied and compared the micro-architectural parameters of bone from the anterior (incisors and canines) and posterior (premolars and molars) regions of 34 adult (18 to 80 years) maxillae. The study made use of micro-CT and found no significant difference in bone volume to total volume ratio (BV/TV) between the anterior and posterior regions of the maxilla (Monje *et al*., 2015). In contrast, Fanuscu and Chang (2004) noted that BV/TV was significantly higher in the anterior region when compared to the posterior region within one individual, aged 72 years. The differences in the bone density in different regions of the maxilla indicate site-specific changes as a result of biomechanical stress and dentition (Devlin *et al*., 1998; Lindh *et al*., 2004). Ulm *et al*. (1999) assessed the features of trabecular micro-architecture of edentulous maxillae in 52 individuals with a mean age of 72.5 years across three regions of the alveolar bone: the lateral incisor, first premolar, and first molar. Trabecular micro-architectural quality decreased from the mesial region to the distal region, with the molar region presenting significantly lower BV/TV, trabecular thickness, and trabecular number measurements (Ulm *et al*., 1999). The significantly lower BV/TV observed by Ulm *et al*. (1999) in the distal region also contrasts results by Monje *et al*. (2015). The three-dimensional (3D) micro-structures that are specific to the maxilla and mandible in juvenile subjects during dental development and eruption have not been described (Mavropoulos *et al*., 2004; Kim *et al*., 2013; Hutchinson *et al*., 2017).

While valuable information on the trabecular micro-architecture of the maxilla is provided in the literature, studies are limited to older age groups (Ulm *et al*., 1999; Fanuscu and Chang, 2004; Monje *et al*., 2015; Kamigaki *et al*., 2017). This limits the depth of inferences which can be made regarding changes in the trabecular micro-architecture that take place during important stages of juvenile growth. These stages include changes in the functionality of structures associated with the maxilla i.e., dental development and eruption as well as general growth of the maxilla.

2 Aim and Objectives

2.1 Aim

To assess changes in the micro-architecture of the alveolar region of the postnatal and subadult human maxilla in relation to dental development and eruption.

2.2 Objectives

1. To evaluate changes in the micro-architecture (bone volume fraction (BV/TV), bone surface to bone volume ration (BS/BV), trabecular thickness (TbTh), trabecular number (TbN), and trabecular spacing (TbSp)) of early postnatal maxillae (individuals with deciduous dentition; 0 – 5 years) across the apical, the buccal, and the lingual surfaces of each dental crypt and compare them to late postnatal maxillae.

2. To assess changes in the micro-architecture (bone volume fraction (BV/TV), bone surface to bone volume ration (BS/BV), trabecular thickness (TbTh), trabecular number (TbN), and trabecular spacing (TbSp)) of the late postnatal maxillae (individuals with mixed dentition; 6 – 12 years) across the apical, the buccal, and the lingual surfaces of each dental crypt and compare them to subadult maxillae.

3. To assess changes in the micro-architecture (bone volume fraction (BV/TV), bone surface to bone volume ration (BS/BV), trabecular thickness (TbTh), trabecular number (TbN), and trabecular spacing (TbSp)) of the subadult (individuals with permanent dentition; 13 – 18 years) maxillae across the apical, the buccal, and the lingual surfaces of each dental crypt.

4. To compare the micro-architecture parameters of the different dentition groups.

3 Materials and methods

3.1 Ethics

The maxillae of the study were used in agreement with the South African National Health Act 61 of 2003. Additionally, permission to use an ethics clearance waiver previously issued to the School of Anatomical Sciences, University of the Witwatersrand was obtained (W-CBP-220504-01) (Appendix A).

3.2 Sample description

Maxillae from a total of 79 individuals were sourced from the Raymond A. Dart Collection of Modern Human Skeletons housed at the School of Anatomical Sciences, University of the Witwatersrand, Johannesburg, South Africa. The individuals used for the purpose of this study were aged between zero and 18 years and were assigned to three dentition groups based on dental development and eruption standards proposed by the London Atlas of Human Tooth Development and Eruption (AlQahtani *et al*., 2010) and the WITS Atlas of Tooth Formation and Emergence (Esan and Schepartz, 2018). The three sample groups included individuals with deciduous dentition only (n=28; F=14 and M=14); 0-5y), mixed dentition (n=9; F=4 and M=5; 6-12y), and permanent dentition only (n=42; F=10 and M=32; 13-18y). Due to the small sample size in the mixed dentition group, the different potential combinations existing within the mixed dentition were not explored i.e., the absence of anterior teeth versus posterior teeth. The population affinity was not assessed in this study, owing to the significant level of genetic admixture in a South African population (Petersen *et al*., 2013; Bajić *et al*., 2018). The study sample consisted predominantly of South African Black (n=73) and South African white (n=3) individuals with a smaller sub-set of individuals categorized as "mixed" (n = 3). In line with research conducted by Bajić *et al*., 2018 where various degrees of genetic admixture were noted in populations from both Northern and Southern Africa as well as the current South African demographic representation, population affinity in the context of the current sample was viewed as a confounding factor. In addition, ancestry was estimated in the juvenile sample from the Raymond A. Dart Collection, and these did not have associated demographics when they were accessioned. It is also extremely difficult to estimate ancestry in juveniles as the expected differences would only develop in adulthood and even though some degree of geographic patterns is observed in morphoscopic characteristics, the level of overlap is very large (Iscan and Steyn, 2013). Individuals were excluded if the maxillae were broken on both the left and the right side or showed any signs of obvious trauma, surgical repair, pathology, and orthodontic treatments.

3.3 Scanning and reconstruction

The maxillae were scanned at the MIXRAD laboratory of the South African Nuclear Energy Corporation (NECSA) using the Nikon XTH 225L micro-focus CT X-ray unit (Nikon Metrology, Leuven, Belgium). To prepare for scanning, the frontal bone of each individual was securely placed in a polystyrene mold, which prevented the movement of the skull during scanning. Subsequent to scanning preparations, the mounted skull was placed onto a rotating sample manipulator to allow for scanning in 360 degrees. The following scanning parameters were put in place: 100 kV/100 µA, at 0.5 frame per second exposure, 1000 projections and 125 µm resolution. The scans were reconstructed using Nikon CTPro software version XT4.4.3 (Nikon Metrology, Leuven, Belgium).

3.4 Analysis of scans

Scans were analyzed using VGStudio V3.2.3 (Volume Graphics GmbH, Heidelberg, Germany). The reconstructed scans were first subjected to a surface determination analysis to enable clear determination of the surface landmarks of each skull. To facilitate the analysis of the dental crypt surfaces, the orientation of the maxillary slices was standardized by aligning every slice with an established plane. A transverse reference plane was established for all scans in order to align the slices to an anatomical plane by selecting four fiducial landmarks along the skull. The fiducial points selected were the right porion, the right nariale, the left nariale, and the left porion (Figure 1).

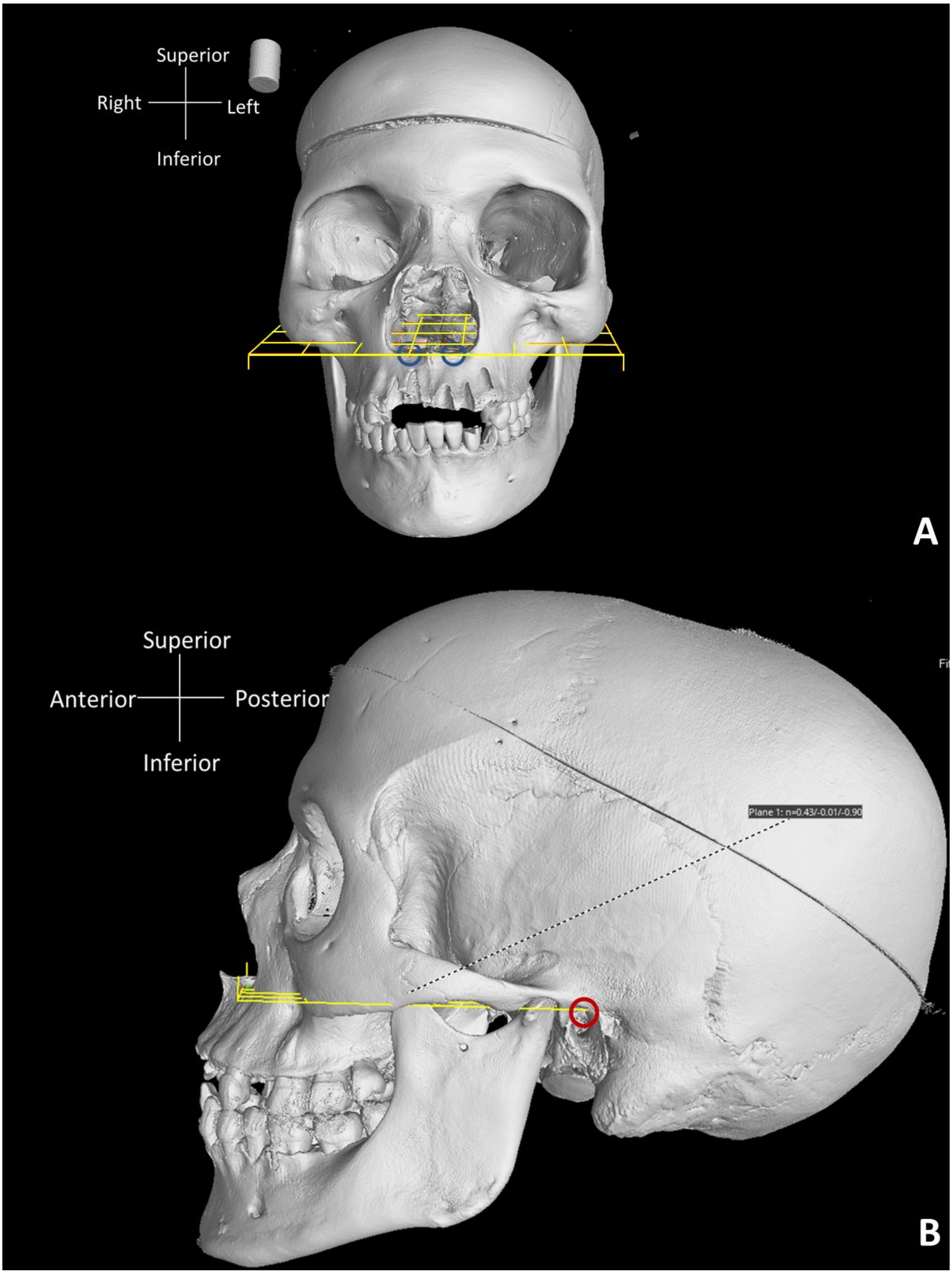

Figure 1 Micro-CT images showing the transverse plane with fiducial points on a skull of an 18-year-old male in anterior (A) and the lateral (B) views. The right and the left nariale are shown by the blue circles in skull A and the left porion is shown by the red circle in skull B. The transverse plane is shown by the red plane in skull A and by the yellow plane in skull B.

All the dental crypts on the left side of the maxilla for each individual were included in this study, with the exception of the third molar crypt. The exclusion of the third molar was because it is the most highly variable amongst individuals in terms of position and timing of dental development and eruption (Narnbiar, 1995; Solari and Abramovitch, 2002; Sisman *et al*., 2007; Sánchez *et al*., 2009; Lewis and Senn, 2010). In cases where the dental crypts on the left side were damaged, the corresponding crypts on the right side were used for analysis. In cases where the teeth were missing on the left side of the maxilla, analysis was conducted providing the crypt was intact. When considering the mixed dentition, in cases where there was a deciduous and a permanent dental crypt, the overall outside border of the two crypts combined was considered (Figure 2).

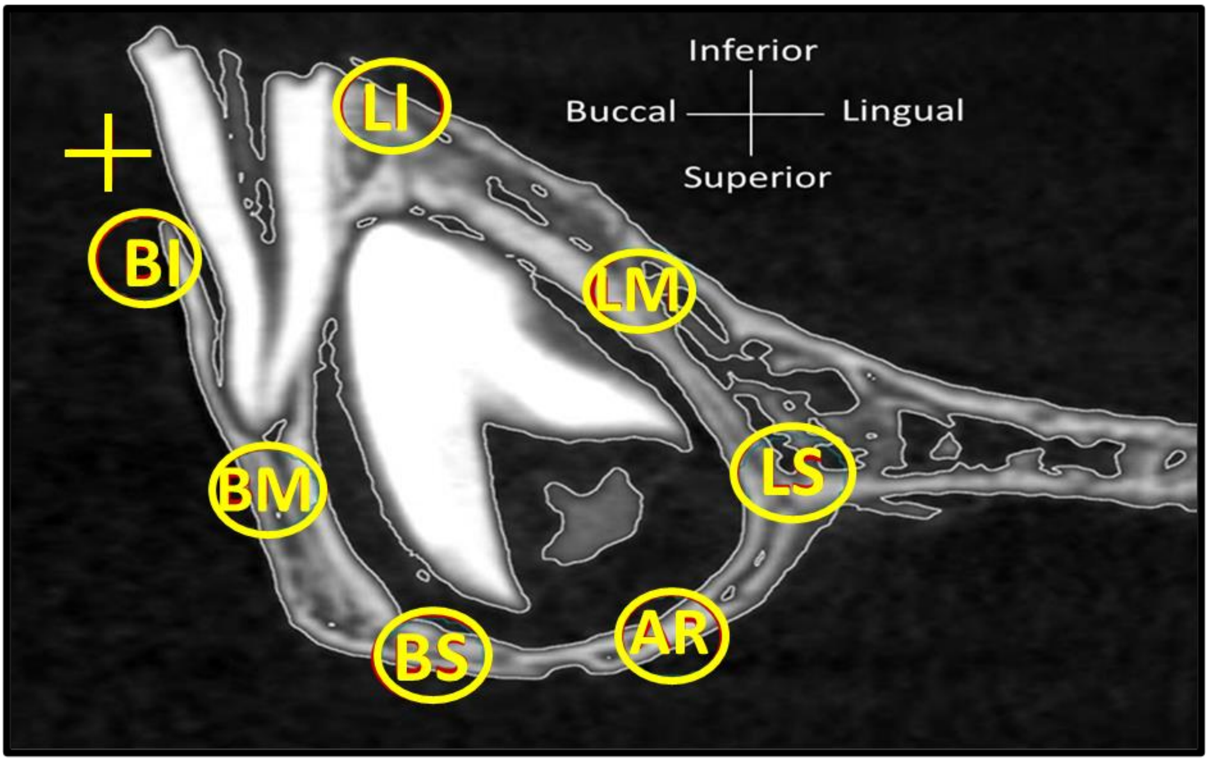

Figure 2 Micro-CT image of a sagittal section through the maxillary central incisor crypt of a 7-year-old male where the deciduous and the permanent incisor crypts were considered collectively. The cross indicates the buccal surface of the maxilla. The seven regions of interest are indicated by the red circles (AR: apex region; BS: buccal superior; BM: buccal middle; BI: buccal inferior; LS: lingual superior; LM: lingual middle; LI: lingual inferior).

To ensure repeatability of obtaining the midpoint sagittal section of each dental crypt, the maximum width (Figure 3, line ab) was first taken at a level where bone was evident across at least three surfaces i.e., between the mesial and the distal surfaces and parallel to the buccal surface of the dental crypt opening of the maxilla across a single cross section. The midpoint (line ac) of the maximum width (line ab) was taken (Figure 3). A 90-degree angle (angle d) was then put in place at the midpoint of the crypt (perpendicular to the maximum width, line ab). This was followed by a buccolingual plane through the crypt aligned with the 90-degree angle, indicated by line e (Figure 3). Slices were aligned with line e to give the sagittal section of each dental crypt. The same measurements in every crypt were taken to find the sagittal plane of the crypts for all the individuals.

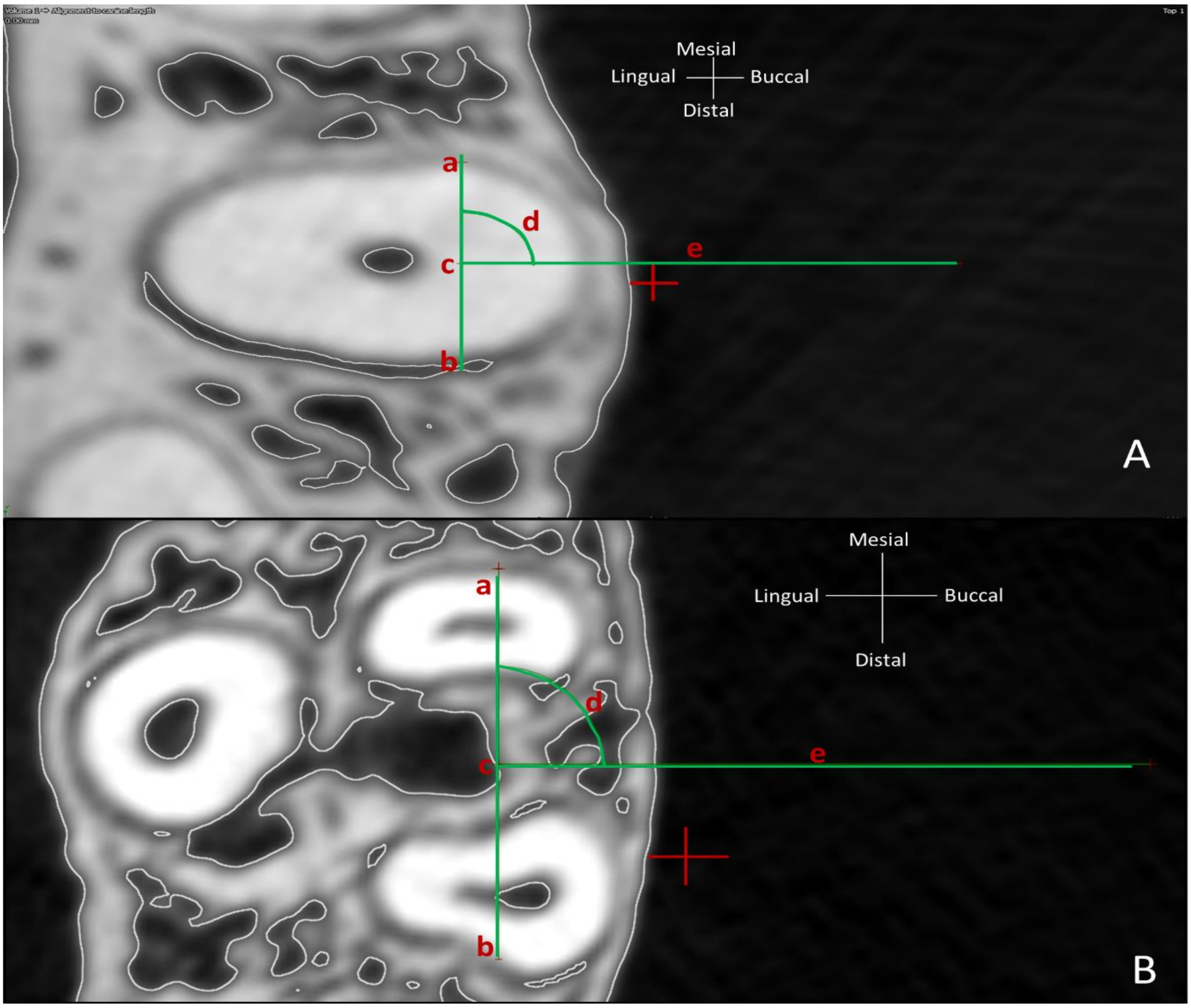

Figure 3 Micro-CT images of a transverse section through the maxillary permanent central incisor (A) and deciduous first molar (B) crypts from the inferior view. The buccal surface is marked by the red cross in both A and B. The line ab is the maximum width of the crypt, point c is the mid-point of the crypt, and the buccolingual plane is marked by line e. The 90-degree angle of the crypt is marked by d.

To analyze the trabecular micro-architecture of the left maxillary dental crypts across the selected sagittal section, the regions of interest (ROI) across the buccal and lingual surfaces of each dental crypt, as well as at the apex were taken. The ROI of each dental crypt included inferior, middle, and superior regions across the buccal and lingual surfaces respectively, and the apex regions (Hutchinson *et al*., 2017). The inferior ROI of each surface was taken at the alveolar bony crest corresponding to the opening of each dental crypt (BI, buccal inferior; LI, lingual inferior, Figure 4B and 4D). In the case of individuals with unerupted teeth, the inferior

ROI was aligned with the crown of the erupting tooth on both the buccal and the lingual sides (Figure 4A and 4C). The superior ROIs of the buccal and the lingual surfaces were aligned with the apical surface of the dental crypt (BS, buccal superior; LS, lingual superior). The middle ROI was taken halfway between the inferior and the superior ROI (BM, buccal middle; LM, lingual middle). The apical ROI was taken at the deepest point on the apex of each dental crypt (AR, apex region). In cases of multirooted teeth where two roots were observed in the sagittal plane, two apical ROI (BA, buccal apex region and LA, lingual apex region) were taken at the deepest point of each root (Figure 4D). The values of all the trabecular micro-architecture parameters of the BA and LA apex ROIs were then averaged to get single apex values for every parameter of every multirooted crypt for comparison across all dental crypts. The diameter as well as the depth of all the ROI were set at 1 mm.

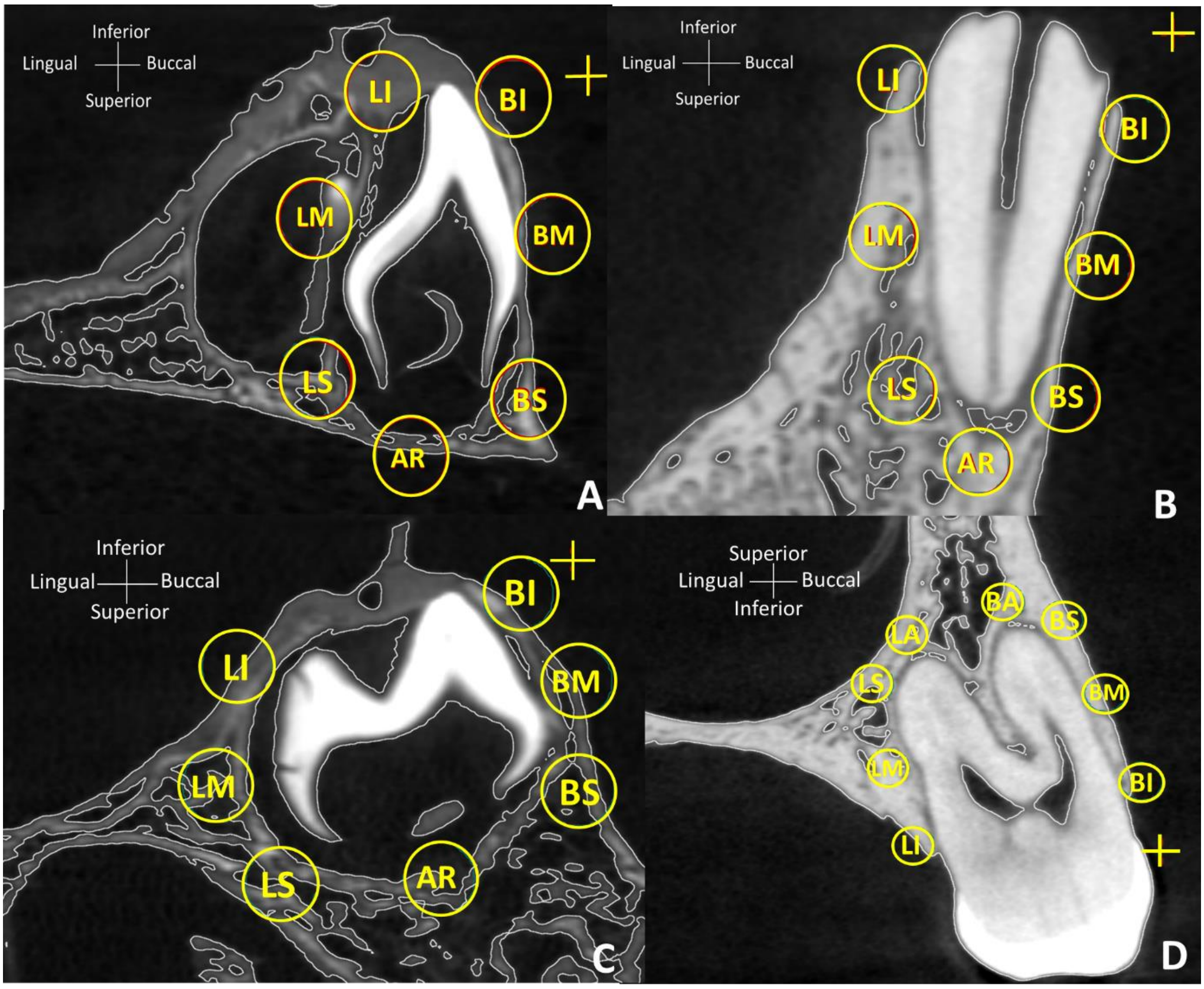

Figure 4 Micro-CT images showing the sagittal section on an unerupted central incisor of a 0-year-old male (A), erupted central incisor of a 17-year-old male (B), unerupted first molar of a 0-year-old male (C) and erupted first premolar of an 18-year-old male (D) crypts. The ROI are marked by the red circles (AR, apex region; LA, lingual apex region; BA, Buccal apex region; LS, lingual superior; LM, lingual middle; LI, lingual inferior; BS, buccal superior; BM, buccal middle, and BI, buccal inferior). The buccal side on all the images is shown by the red cross.

The internal micro-architecture of the bone at each region of interest of every dental crypt was investigated using trabecular number (1/mm), trabecular thickness (mm), trabecular spacing (mm), material surface to material volume (BS/BV), and bone volume to total volume ratio (BV/TV). Trabecular number (TbN) refers to the number of trabeculae found within a selected region of the bone. Trabecular thickness (TbTh) is the average thickness of trabeculae in a selected region on the bone. Trabecular spacing or separation (TbSp) is the average distance between trabeculae (Parfitt, 1988; Stauber and Müller, 2008; Blok *et al*., 2013). Material surface to material volume ratio (BS/BV) is the amount of surface area per unit volume of bone sample (Fan *et al*., 2011). BV/TV measures the amount of mineralized bone per unit volume of the total bone sample (Klintström *et al*., 2014).

3.5 Data entry, management, and repeatability

Collected data was entered into Microsoft Excel (Microsoft Corporation, New Mexico, United States) and analyzed using IBM SPSS Statistics v.28.0 (IBM, Armonk, NY, USA) and R Studio v.4.2.2 (Posit Software, PBC, Boston, USA). Levels of repeatability were evaluated using two methods for comparison purposes: Lin's concordance correlation coefficient of reproducibility (Lawrence and Lin, 1989) and technical error of measurement (TEM) (Langley *et al*., 2018). For intra-observer repeatability, trabecular parameters from 9 individuals (10% of the total sample) selected from all the dentition groups across the sample were measured by the primary observer and were repeated a week later. For inter-observer error repeatability, both the primary and the secondary (supervisor) observers measured the same trabecular parameters from the same 9 individuals and the results were used to determine the inter-observer error. Repeatability and reliability values of more than 0.90 were considered excellent (Allan, 1982).

3.6 Statistical analysis

A Shapiro-Wilk's test was used to assess the distribution of the data. The distribution type then determined which statistical analyses were used. The data was found to be non-parametric ($p \leq 0.001$) and therefore the median and an interquartile range were calculated for all the assessed trabecular micro-architecture parameters. Analysis of variance (ANOVA) and Tukey's post hoc test were done to compare the trabecular parameters between dental crypts for each of the assessed maxillary surfaces within each age group. Furthermore, a multivariate ANOVA was done to evaluate the level of interaction between age group and trabecular micro-architecture parameters. This was followed by Tukey's post hoc test and pairwise comparisons between dentition groups to assess the nature of the differences in trabecular micro-architecture. A p-value of less than 0.05 was considered statistically significant.

4 Results

High levels of repeatability were observed for intra-observer error (82.9%-97.1%) and inter-observer error (73.9%-96.4%) for all the trabecular parameters except for TbTh where the lowest repeatability was 46.3% for inter-observer and 49.9% for intra-observer (Table 13 – 17, Appendix B). Using TEM, moderate to high levels of repeatability were observed for intra-observer (66.9%-93.1%) and inter-observer (71.4%-87.4%) and the lowest values for both intra- and inter-observer error were observed in TbTh (Table 18 and 19, Appendix B).

4.1 Patterns of changes in trabecular micro-architecture

When comparing the internal micro-architectural parameters across each of the dentition groups, the TbSp, BV/TV and TbTh all showed increases with the advancement of dentition stages, i.e., as dentition develops and erupts, these parameters showed an increase. TbN and BS/BV both appeared to decrease when comparing across dentition groups were compared (Table 1)

Table 1 The means (SD) of trabecular parameters (BV/TV, BS/BV, TbTh, TbN, and TbSp) between the deciduous dentition group, mixed dentition group, and permanent dentition group.

	BV/TV	**BS/BV**	**TbTh**	**TbN**	**TbSp**
Deciduous (n = 28)	0.46 (0.03)	4.26 (0.25)	0.85 (0.06)	0.74 (0.03)	1.02 (0.06)
Mixed (n = 9)	0.47 (0.03)	3.41 (0.29)	1.24 (0.16)	0.66 (0.03)	1.10 (0.05)
Permanent (n = 42)	0.57 (0.04)	2.29 (0.21)	3.72 (0.35)	0.48 (0.03)	1.21 (0.05)

BV/TV: bone volume fraction; BV/BS: material surface to material volume fraction; TbTh: Trabecular thickness; TbN: trabecular number; TbSp: Trabecular spacing. SD: standard deviation.

In the assessment of internal parameter changes across each of the dentition sets, BV/TV was significantly higher ($p \leq 0.01$) in the permanent dentition group when compared to the mixed dentition group (Table 2). The BS/BV parameter was significantly higher in the mixed dentition group when compared to permanent dentition group ($p \leq 0.01$) as well as in the deciduous dentition group when compared to the mixed dentition group ($p \leq 0.01$). The TbN in the permanent dentition group was significantly higher than the mixed dentition group ($p \leq 0.01$). In addition, the trabecular number in the mixed dentition group was also significantly higher when compared to the deciduous dentition group ($p \leq 0.01$) (Table 2). No statistically significant differences were observed when assessing micro-architectural changes between the deciduous, mixed, and the permanent dentition groups respectively across the TbTh and TbSp parameters (Table 2).

Table 2 Analysis of variance (ANOVA) and Tukey's post hoc test indicating the differences in the five trabecular micro-architecture parameters (BV/TV, BS/BV, TbTh, TbN, and TbSp) between the deciduous, mixed, and permanent dentition groups.

Dependent variable	Univariate ($p<0.05$)	Group	Group	Pairwise comparison ($p<0.05$)
BV/TV	≤0.01*	Deciduous	Mixed	≤0.95
		Mixed	Permanent	≤0.01*
BS/BV	≤0.01*	Deciduous	Mixed	≤0.01*
		Mixed	Permanent	≤0.01*
TbTh	≤0.22	Deciduous	Mixed	≤1.00
		Mixed	Permanent	≤0.48
TbN	≤0.01*	Deciduous	Mixed	≤0.01*
		Mixed	Permanent	≤0.01*
TbSp	≤0.05	Deciduous	Mixed	≤0.38
		Mixed	Permanent	≤0.93

BV/TV: bone volume fraction; BS/BV: material surface to material volume ratio; TbTh: trabecular thickness; TbN: trabecular number; TbSp: trabecular spacing. Values marked with an asterisk (*) are values that were significantly lower than 0.001 and were presented as p≤0.01.

4.2 Bone micro-architecture variables

4.2.1 Bone micro-architecture variables between dentition groups

No significant differences were found in the BV/TV ratio between the dental crypts of the deciduous and the mixed dentition groups. A significantly higher ($p \le 0.03$) BV/TV ratio was found on the apical region of the central incisor of the permanent dentition when compared to the central incisor of the mixed dentition (Table 3, Figure 5C and 5E).

No significant differences were found in BS/BV between the dental crypts of deciduous and mixed dentition groups. A significantly higher BS/BV was found on the apical region of the mixed dentition central incisor ($p \le 0.04$) and lateral incisor ($p \le 0.02$) when compared to the apical region of the same dental crypts in the permanent dentition respectively (Table 4, Figure 5C and 5E).

No significant differences were found in TbTh of dental crypts between dentition groups (Table 5).

The lingual side of the canine dental crypt of the deciduous dentition had significantly more trabeculae (TbN, $p \le 0.04$) when compared to the lingual side of the canine of the mixed dentition (Table 6). No other significant differences were found between the remaining crypts of the deciduous and the mixed dentition groups. Across the apical ($p \le 0.04$), the buccal ($p \le 0.01$), and the lingual ($p \le 0.01$) areas of the central incisor crypt within the mixed dentition, there was significantly more trabeculae (TbN) when compared to the central incisor crypt of the permanent dentition group (Table 6, Figure 5C and 5E). The apical region of the canine crypt of the mixed dentition had a significantly higher ($p \le 0.04$) TbN when compared to the apical region of the canine crypt of the permanent dentition (Table 6). In the mixed dentition group, a significantly higher TbN was found across the buccal ($p \leq 0.03$) and lingual ($p \leq 0.02$) sides of the first molar compared to permanent dentition first molar (Table 6).

While no statistically significant differences were found in TbSp of dental crypts between the dentition age groups (Table 7), the lingual sides of both the central incisor and the lateral incisor were visibly more porous in the mixed dentition when compared to the permanent dentition (Figure 5C and 5D compared to 5E and 5F, respectively).

Table 3 Analysis of variance (ANOVA) indicating pairwise comparisons of BV/TV for each dental crypt surface between dentition groups.

	Apical				Buccal				Lingual			
	Univariate (p<0.05)	Deciduous vs. Mixed	Univariate (p<0.05)	Mixed vs. Permanent	Univariate (p<0.05)	Deciduous vs. Mixed	Univariate (p<0.05)	Mixed vs. Permanent	Univariate (p<0.05)	Deciduous vs. Mixed	Univariate (p<0.05)	Mixed vs. Permanent
Central incisor	≤0.03	0.99	≤0.01*	0.003	≤0.02*	0.31	≤0.01*	0.90	≤ 0.65	1.00	≤0.04	0.99
Lateral incisor	≤0.03	0.89	≤0.01*	0.11	≤0.02*	0.72	≤0.01*	1.00	≤ 0.65	1.00	≤0.04	0.97
Canine	≤0.03	1.00	≤0.01*	0.92	≤0.02*	1.00	≤0.01*	0.99	≤0.65	1.00	≤0.04	1.00
Deciduous molar 1	≤0.03	1.00	≤0.01*	-	≤0.02*	0.99	≤0.01*	-	≤0.65	1.00	-	-
Deciduous molar 2	≤0.03	1.00	≤0.01*	-	≤0.02*	0.93	≤0.01*	-	≤0.65	1.00	-	-
Permanent molar 1	≤0.03	0.99	≤0.01*	0.53	≤0.02*	1.00	≤0.01*	0.07	≤0.65	1.00	≤0.04	0.22
Permanent molar 2	-	-	-	-	-	-	-	-	-	-	-	-

*BV/TV is the bone volume fraction. Deciduous (n = 28; 0 – 5 years); Mixed (n = 9; 6 – 12 years); Permanent (n = 42; 13 – 18 years). * The values were significantly lower than 0.001 and were represented as p≤0.01.*

Table 4 Analysis of variance (ANOVA) indicating pairwise comparisons of BS/BV for each dental crypt surface between dentition groups.

	Apical				Buccal				Lingual			
	Univariate (p<0.05)	Deciduous vs. Mixed	Univariate (p<0.05)	Mixed vs. Permanent	Univariate (p<0.05)	Deciduous vs. Mixed	Univariate (p<0.05)	Mixed vs. Permanent	Univariate (p<0.05)	Deciduous vs. Mixed	Univariate (p<0.05)	Mixed vs. Permanent
Central incisor	≤0.06	1.00	≤0.01*	0.04	≤0.01*	0.99	≤0.01	1.00	≤0.01*	0.99	≤0.01*	0.05
Lateral incisor	≤0.06	0.84	≤0.01*	0.02	≤0.01*	1.00	≤0.01	0.74	≤0.01*	1.00	≤0.01*	0.73
Canine	≤0.06	1.00	≤0.01*	0.78	≤0.01*	0.39	≤0.01	1.00	≤0.01*	0.77	≤0.01*	1.00
Deciduous molar 1	≤0.06	0.97	-	-	≤0.01*	0.61	-	-	≤0.01*	0.21	-	-
Deciduous molar 2	≤0.06	1.00	-	-	≤0.01*	0.75	-	-	≤0.01*	0.51	-	-
Permanent molar 1	≤0.06	0.70	≤0.01*	0.98	≤0.01*	0.28	≤0.01	0.01	≤0.01*	0.88	≤0.01*	0.09
Permanent molar 2	-	-	-	-	-	-	-	-	-	-	-	-

*BS/BV is the bone surface to bone volume ratio. Deciduous (n = 28; 0 – 5 years); Mixed (n = 9; 6 – 12 years); Permanent (n = 42; 13 – 18 years). *The values were significantly lower than 0.001 and were represented as p≤0.01.*

Table 5 Analysis of variance (ANOVA) indicating pairwise comparisons of TbTh for each dental crypt surface between dentition groups.

	Apical				Buccal				Lingual			
	Univariate (p<0.05)	Deciduous vs. Mixed	Univariate (p<0.05)	Mixed vs. Permanent	Univariate (p<0.05)	Deciduous vs. Mixed	Univariate (p<0.05)	Mixed vs. Permanent	Univariate (p<0.05)	Deciduous vs. Mixed	Univariate (p<0.05)	Mixed vs. Permanent
Central incisor	≤0.39	1.00	≤0.93	0.99	≤0.78	1.00	≤0.03	1.00	≤0.32	1.00	≤0.37	0.89
Lateral incisor	≤0.39	0.12	≤0.93	1.00	≤0.78	0.98	≤0.03	1.00	≤0.32	1.00	≤0.37	1.00
Canine	≤0.39	1.00	≤0.93	1.00	≤0.78	1.00	≤0.03	1.00	≤0.32	0.21	≤0.37	1.00
Deciduous molar 1	≤0.39	1.00	-	-	≤0.78	1.00	-	-	≤0.32	1.00	-	-
Deciduous molar 2	≤0.39	1.00	-	-	≤0.78	1.00	-	-	≤0.32	1.00	-	-
Permanent molar 1	≤0.39	1.00	≤0.93	1.00	≤0.78	1.00	≤0.03	0.66	≤0.32	1.00	≤0.37	1.00
Permanent molar 2	-	-	-	-	-	-	-	-	-	-	-	-

TbTh is the trabecular thickness of a selected region on the bone. Deciduous (n = 28; 0 – 5 years); Mixed (n = 9; 6 – 12 years); Permanent (n = 42; 13 – 18 years).

.

Table 6 Analysis of variance (ANOVA) indicating pairwise comparisons of TbN for each dental crypt surface between dentition groups.

	Apical				Buccal				Lingual			
	Univariate (p<0.05)	Deciduous vs. Mixed	Univariate (p<0.05)	Mixed vs. Permanent	Univariate (p<0.05)	Deciduous vs. Mixed	Univariate (p<0.05)	Mixed vs. Permanent	Univariate (p<0.05)	Deciduous vs. Mixed	Univariate (p<0.05)	Mixed vs. Permanent
Central incisor	≤0.02	0.98	≤0.01*	0.04	≤0.01*	0.97	≤0.01*	0.01	≤0.01*	0.99	≤0.01*	≤0.01*
Lateral incisor	≤0.02	0.71	≤0.01*	1.00	≤0.01*	0.99	≤0.01*	0.38	≤0.01*	1.00	≤0.01*	0.99
Canine	≤0.02	1.00	≤0.01*	0.04	≤0.01*	0.65	≤0.01*	0.96	≤0.01*	0.04	≤0.01*	0.97
Deciduous molar 1	≤0.02	0.99	-	-	≤0.01*	0.99	-	-	≤0.01*	0.13	-	-
Deciduous molar 2	≤0.02	0.99	-	-	≤0.01*	1.00	-	-	≤0.01*	0.47	-	-
Permanent molar 1	≤0.02	0.99	≤0.01*	1.00	≤0.01*	0.99	≤0.01*	0.03	≤0.01*	0.96	≤0.01*	≤0.02
Permanent molar 2	-	-	-	-	-	-	-	-	-	-	-	-

*TbN is the number of trabeculae found in a selected area of bone. Deciduous (n = 28; 0 – 5 years); Mixed (n = 9; 6 – 12 years); Permanent (n = 42; 13 – 18 years). *The values were significantly lower than 0.001 and were presented as p≤0.01.*

Table 7 Analysis of variance (ANOVA) indicating pairwise comparisons of TbSp for each dental crypt surface between dentition groups.

	Apical				Buccal				Lingual			
	Univariate (p<0.05)	Deciduous vs. Mixed	Univariate (p<0.05)	Mixed vs. Permanent	Univariate (p<0.05)	Deciduous vs. Mixed	Univariate (p<0.05)	Mixed vs. Permanent	Univariate (p<0.05)	Deciduous vs. Mixed	Univariate (p<0.05)	Mixed vs. Permanent
Central incisor	≤0.01	0.47	≤0.99	1.00	≤0.03*	0.59	≤0.01	0.27	≤0.01	0.22	≤0.04	0.99
Lateral incisor	≤0.01	0.58	≤0.99	1.00	≤0.03*	0.99	≤0.01	1.00	≤0.01	1.00	≤0.04	1.00
Canine	≤0.01	1.00	≤0.99	1.00	≤0.03*	0.99	≤0.01	0.94	≤0.01	0.97	≤0.04	1.00
Deciduous molar 1	≤0.01	1.00	-	-	≤0.03*	1.00	-	-	≤0.01	0.34	-	-
Deciduous molar 2	≤0.01	0.99	-	-	≤0.03*	1.00	-	-	≤0.01	0.72	-	-
Permanent molar 1	≤0.01	1.00	≤0.99	1.00	≤0.03*	1.00	≤0.01	1.00	≤0.01	0.59	≤0.04	1.00
Permanent molar 2	-	-	-	-	-	-	-	-	-	-	-	-

TbSp is the trabecular spacing found in a selected region of bone. Deciduous (n = 28; 0 – 5 years); Mixed (n = 9; 6 – 12 years); Permanent (n = 42; 13 – 18 years). The values 0.01 and 0.03 were significantly lower than 0.001 and 0.003 and were presented as p≤0.01 and p≤0.03, respectively.

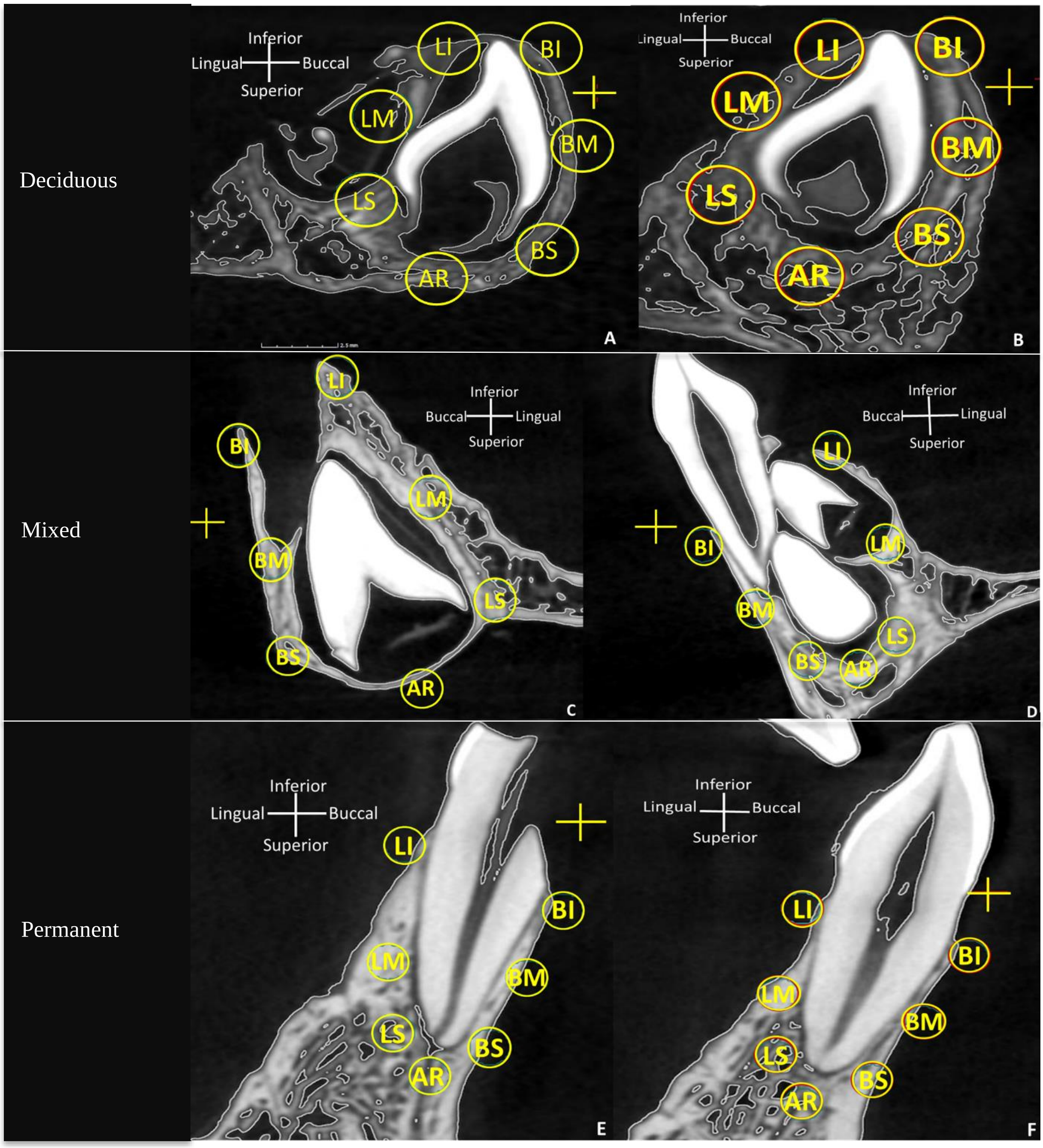

Figure 5 Micro-CT images showing the sagittal sections of central incisors (A, C, E) and lateral incisors (B, D, F) from the deciduous, mixed, and permanent dentition groups, respectively. The buccal sides are indicated by the red crosses. The ROI are marked by the red circles (AR, apex region; LA, lingual apex region; BA, Buccal apex region; LS, lingual superior; LM, lingual middle; LI, lingual inferior; BS, buccal superior; BM, buccal middle, and BI, buccal inferior).

4.2.2 Bone micro-architecture variables within each dentition group

In the deciduous dentition, a significantly higher BV/TV ratio was found across both the apical ($p \leq 0.01$) and the buccal ($p \leq 0.01$) areas of the lateral incisor dental crypt when compared to the central incisor dental crypt (Table 8, Figure 5). The amount of bone expressed as BV/TV, was greater in the lateral incisor (Figure 5B) when compared to the central incisor (Figure 5A). The BV/TV ratio on the buccal surface of the lateral incisor was also significantly higher ($p \leq 0.06$) when compared to the buccal side of the canine crypt in the deciduous dentition (Table 8). While no significant differences were observed within the mixed dentition group when comparing across the individual dental crypts, a significantly higher ratio of BV/TV ($p \leq 0.01$) was observed on the buccal side of the second premolar crypt compared to the first premolar crypt in the permanent dentition (Table 8).

The BS/BV ratio was found to be significantly higher ($p \leq 0.02$) on the buccal side of the canine dental crypt compared to the first premolar dental crypt in the permanent dentition (Table 9). No other significant differences were observed in BS/BV within each dentition group. No significant differences were found in TbTh between crypts within each dentition group (Table 10).

The apical region of the lateral incisor crypt of the deciduous dentition had a significantly higher ($p \leq 0.01$) TbN when compared to the central incisor crypt (Table 11). Trabeculae were found to be significantly higher ($p \leq 0.02$) on the lingual side of the canine dental crypt when compared to the lingual side of the lateral incisor crypt in the deciduous dentition (Table 11). The TbN was also found to be significantly higher on the apical region of the lateral incisor crypt when compared to the apical regions of the central incisor crypt ($p \leq 0.02$) and the canine crypt ($p \leq 0.02$) in the permanent dentition (Table 11). In the permanent dentition, the buccal

($p \leq 0.01$) and the lingual ($p \leq 0.01$) sides of the second premolar crypt had a significantly higher TbN when compared to the first molar crypt (Table 11).

Across the apical ($p \leq 0.01$), the buccal ($p \leq 0.02$) and the lingual ($p \leq 0.02$) areas of the central incisor crypt, there was significantly more spacing (TbSp) when compared to the lateral incisor crypt in the deciduous dentition (Table 12, Figure 5). The TbSp was also found to be significantly higher ($p \leq 0.04$) on the lingual side of the lateral incisor crypt when compared to the canine crypt in the deciduous dentition (Table 12). In the permanent dentition group, the buccal side of the first premolar crypt had a significantly higher ($p \leq 0.04$) TbSp when compared to the buccal side of the second premolar crypt (Table 12).

Table 8 Analysis of variance (ANOVA) indicating pairwise comparisons of BV/TV for each dental crypt surface across dentition groups associated with the deciduous dentition, the mixed dentition, and the permanent dentition respectively.

	Median ± IQR										Pairwise comparisons (p<0.05)					
	CI	**LI**	**C**	**DM1**	**DM2**	**PM1**	**PM2**	**M1**	**M2**	**Univariate p<0.05**	**CI vs. LI**	**LI vs. C**	**C vs D/PM 1**	**D/PM 1 vs. D/PM 2**	**D/PM 2 vs. M1**	**M1 vs. M2**
Deciduous (n = 28; 0 – 5 years)																
AA	0.58 ± 0.37	0.64 ± 0.23	0.52 ± 0.31	0.51 ± 0.24	0.41 ± 0.32	-	-	0.21 ± 0.32	-	≤0.01*	≤0.01*	0.76	0.98	0.82	0.84	-
BA	0.23 ± 0.16	0.50 ± 0.31	0.37 ± 0.24	0.38 ± 0.11	0.32 ± 0.23	-	-	0.37 ± 0.24	-	≤0.01*	≤0.01*	0.06	0.95	0.99	1.00	-
LA	0.58 ± 0.24	0.51 ± 0.26	0.52 ± 0.19	0.48 ± 0.22	0.47 ± 0.33	-	-	0.47 ± 0.40	-	≤0.21	0.80	0.42	0.24	1.00	1.00	-
Mixed (n = 9; 6 -12 years)																
AA	0.52 ± 0.35	0.49 ± 0.51	0.65 ± 0.23	0.54 ± 0.24	0.35 ± 0.28	-	-	0.36 ± 0.31	-	≤0.44	1.00	0.91	0.99	0.97	1.00	-
BA	0.44 ± 0.19	0.43 ± 0.29	0.44 ± 0.12	0.40 ± 0.17	0.52 ± 0.24	-	-	0.43 ± 0.20	-	≤0.96	0.95	0.99	1.00	1.00	1.00	-
LA	0.55 ± 0.19	0.49 ± 0.25	0.52 ± 0.27	0.45 ± 0.27	0.47 ± 0.24	-	-	0.45 ± 0.15	-	≤0.69	0.99	0.99	0.93	1.00	1.00	-
Permanent (n = 42; 13 – 18 years)																
AA	0.91 ± 0.20	0.80 ± 0.30	0.84 ± 0.40	-	-	0.70 ± 0.31	0.62 ± 0.35	0.63 ± 0.34	0.60 ± 0.26	≤0.01	0.28	0.99	0.94	0.66	1.00	1.00
BA	0.36 ± 0.25	0.42 ± 0.24	0.34 ± 0.23	-	-	0.36 ± 0.22	0.54 ± 0.27	0.66 ± 0.25	0.65 ± 0.29	≤0.01*	0.44	0.82	0.99	0.01	0.25	0.99
LA	0.65 ± 0.15	0.57 ± 0.19	0.60 ± 0.19	-	-	0.58 ± 0.22	0.57 ± 0.18	0.62 ± 0.19	0.59 ± 0.21	≤0.85	0.72	0.99	1.00	1.00	1.00	1.00

*BV/TV is the bone volume fraction. IQR: Interquartile range; CI: Central incisor; LI: Lateral incisor; C: Canine; DM1: Deciduous molar 1; DM2: Deciduous molar 2; PM1: Premolar 1; PM2: Premolar 2; M1: Molar 1; M2: Molar 2; AA: Apical average; BA: Buccal average; LA: Lingual average. *The values were significantly lower than 0.001 and were therefore presented as p≤0.01.*

Table 9 Analysis of Variance (ANOVA) indicating pairwise comparisons of BS/BV for each dental crypt surface across dentition groups associated with the deciduous dentition, the mixed dentition, and the permanent dentition respectively.

	Median ± IQR										Pairwise comparison (p<0.05)					
	CI	LI	C	DM1	DM2	PM1	PM2	M1	M2	Univariate p<0.05	CI vs. LI	LI vs. C	C vs D/PM1	D/PM1 vs. D/PM2	D/PM2 vs. M1	M1 vs. M2
Deciduous (n = 28; 0 – 5 years)																
AA	3.89 ± 2.35	3.32 ± 2.58	3.86 ± 2.35	4.46 ± 2.94	5.44 ± 3.60	-	-	5.26 ± 6.15	-	≤0.27	0.59	1.00	0.51	0.95	0.99	-
BA	4.49 ± 1.99	3.07 ± 2.17	4.20 ± 2.89	3.85 ± 2.15	5.96 ± 3.57	-	-	5.52 ± 4.51	-	≤0.04	0.56	0.56	1.00	0.19	1.00	-
LA	2.89 ± 2.02	3.32 ± 2.25	3.86 ± 2.29	3.79 ± 2.97	3.94 ± 3.04	-	-	4.12 ± 4.59	-	≤0.02	0.95	0.96	0.62	1.00	1.00	-
Mixed (n = 9; 6 – 12 years)																
AA	3.54 ± 2.96	4.28 ± 6.05	2.66 ± 1.42	3.86 ± 1.60	5.14 ± 4.66	-	-	3.80 ± 3.30	-	≤0.82	0.99	0.83	1.00	0.99	1.00	-
BA	3.20 ± 1.88	3.16 ± 2.07	2.51 ± 1.11	2.76 ± 1.80	3.54 ± 4.59	-	-	3.58 ± 2.47	-	≤0.42	1.00	0.97	1.00	0.59	0.98	-
LA	3.56 ± 2.36	3.09 ± 1.87	2.74 ± 1.99	2.92 ± 1.54	3.07 ± 1.03	-	-	2.78 ± 0.85	-	≤0.70	1.00	0.92	1.00	1.00	0.99	-
Permanent (n = 42; 13 – 18 years)																
AA	0.81 ± 1.64	1.82 ± 2.96	1.32 ± 2.68	-	-	2.09 ± 1.79	2.55 ± 2.35	2.89 ± 2.54	2.69 ± 2.07	≤0.01*	0.08	0.38	0.93	0.75	0.89	0.98
BA	2.71 ± 1.48	2.21 ± 1.43	2.60 ± 1.72	-	-	2.16 ± 0.96	1.61 ± 1.05	1.92 ± 2.02	1.75 ± 1.32	≤0.01*	0.20	0.69	0.02	0.76	0.90	1.00
LA	2.07 ± 1.52	2.30 ± 1.58	2.29 ± 2.02	-	-	1.85 ± 1.41	2.38 ± 1.58	1.47 ± 1.17	1.61 ± 1.05	≤0.01*	0.85	1.00	0.82	1.00	0.19	1.00

*BS/BV is the bone surface to bone volume ratio. IQR: Interquartile range; CI: Central incisor; LI: Lateral incisor; C: Canine; DM1: Deciduous molar 1; DM2: Deciduous molar 2; PM1: Premolar 1; PM2: Premolar 2; M1: Molar 1; M2: Molar 2; AA: Apical average; BA: Buccal average; LA: Lingual average. *The values were significantly lower than 0.001 and were presented as p≤0.01.*

Table 10 Analysis of variance (ANOVA) indicating pairwise comparisons of TbTh for each dental crypt surface across dentition groups associated with the deciduous dentition, the mixed dentition, and the permanent dentition respectively.

	Median ± IQR										Pairwise comparison (p<0.05)					
	CI	**LI**	**C**	**DM1**	**DM2**	**PM1**	**PM2**	**M1**	**M2**	**Univariate p<0.05**	**CI vs. LI**	**LI vs. C**	**C vs D/PM 1**	**D/PM1 vs. D/PM2**	**D/PM 2 vs. M1**	**M1 vs. M2**
Deciduous (n = 28; 0 – 5 years)																
AA	0.52 ± 0.24	0.61 ± 0.45	0.51 ± 0.46	0.45 ± 0.34	0.37 ± 0.23	-	-	0.35 ± 0.23	-	≤0.45	0.99	1.00	0.97	0.98	0.99	-
BA	0.48 ± 0.25	0.92 ± 0.91	0.51 ± 0.43	0.64 ± 0.32	0.37 ± 0.25	-	-	0.40 ± 0.26	-	≤0.25	0.32	0.37	1.00	1.00	1.00	-
LA	0.91 ± 0.65	0.68 ± 0.53	0.61 ± 0.33	0.64 ± 0.45	0.58 ± 0.65	-	-	0.59 ± 0.78	-	≤0.31	1.00	0.41	1.00	1.00	1.00	-
Mixed (n = 9; 6 – 12 years)																
AA	0.50 ± 0.44	0.46 ± 0.79	0.76 ± 0.29	0.58 ± 0.25	0.38 ± 0.41	-	-	0.62 ± 0.58	-	≤0.83	0.82	0.88	1.00	1.00	1.00	-
BA	0.71 ± 0.60	0.76 ± 0.68	0.95 ± 0.49	0.75 ± 0.60	0.67 ± 0.58	-	-	0.58 ± 0.38	-	≤0.73	1.00	1.00	0.99	1.00	1.00	-
LA	0.67 ± 0.19	0.90 ± 0.46	0.77 ± 0.66	0.83 ± 0.54	0.78 ± 0.21	-	-	0.80 ± 0.37	-	≤0.88	1.00	0.98	0.97	1.00	1.00	-
Permanent (n = 42; 13 -18 years)																
AA	1.92 ± 3.70	1.06 ± 1.58	0.94 ± 2.73	-	-	1.00 ± 1.35	0.88 ± 1.04	0.75 ± 1.10	0.80 ± 0.69	≤0.38	0.44	1.00	1.00	1.00	1.00	1.00
BA	0.81 ± 0.58	1.11 ± 0.70	0.95 ± 0.68	-	-	1.06 ± 0.55	1.47 ± 1.00	1.30 ± 1.50	1.30 ± 1.02	≤0.01	0.99	1.00	1.00	0.80	0.97	1.00
LA	1.26 ± 1.65	1.34 ± 1.18	1.17 ± 1.60	-	-	1.52 ± 1.27	1.05 ± 0.70	1.84 ± 0.97	1.57 ± 1.27	≤0.26	0.66	0.99	0.99	0.39	0.92	1.00

TbTh is the trabecular thickness of trabeculae in a selected region of bone. IQR: Interquartile range; CI: Central incisor; LI: Lateral incisor; C: Canine; DM1: Deciduous molar 1; DM2: Deciduous molar 2; PM1: Premolar 1; PM2: Premolar 2; M1: Molar 1; M2: Molar 2; AA: Apical average; BA: Buccal average; LA: Lingual average.

Table 11 Analysis of variance (ANOVA) indicating pairwise comparisons of TbN for each dental crypt surface across dentition groups associated with the deciduous dentition, the mixed dentition, and the permanent dentition respectively.

Median ± IQR											Pairwise comparison (p<0.05)					
	CI	**LI**	**C**	**DM1**	**DM2**	**PM1**	**PM2**	**M1**	**M2**	**Univariate p<0.05**	**CI vs. LI**	**LI vs. C**	**C vs D/P M1**	**D/P M1 vs. D/P M2**	**D/P M2 vs. M1**	**M1 vs M2**
Deciduous (n = 28; 0 – 5 years)																
AA	0.59 ± 0.41	1.05 ± 0.50	0.95 ± 0.40	1.04 ± 0.52	1.00 ± 0.51	-	-	0.99 ± 0.65	-	≤0.01	0.01	0.94	0.95	1.00	0.99	-
BA	0.45 ± 0.20	0.58 ± 0.37	0.59 ± 0.29	0.69 ± 0.46	0.71 ± 0.61	-	-	0.89 ± 0.26	-	≤0.01	0.51	0.99	0.93	0.66	0.98	-
LA	0.75 ± 0.26	0.68 ± 0.29	0.90 ± 0.26	0.77 ± 0.32	0.76 ± 0.41	-	-	0.75 ± 0.33	-	≤0.03	0.86	≤0.02	0.82	1.00	1.00	-
Mixed (n = 9; 6 – 12 years)																
AA	0.83 ± 0.38	0.97 ± 0.58	0.96 ± 0.26	0.89 ± 0.34	0.77 ± 0.29	-	-	0.69 ± 0.16	-	≤0.69	0.98	0.98	1.00	1.00	1.00	-
BA	0.55 ± 0.29	0.44 ± 0.40	0.40 ± 0.27	0.64 ± 0.31	0.86 ± 0.16	-	-	0.78 ± 0.21	-	≤0.01	0.98	0.99	0.97	0.42	0.99	-
LA	0.83 ± 0.32	0.66 ± 0.24	0.67 ± 0.26	0.54 ± 0.25	0.58 ± 0.28	-	-	0.69 ± 0.21	-	≤0.03	0.23	1.00	0.99	1.00	0.99	-
Permanent (n = 42; 13 – 18 years)																
AA	0.36 ± 0.55	0.70 ± 0.68	0.41 ± 0.63	-	-	0.62 ± 0.41	0.69 ± 0.42	0.82 ± 0.54	0.77 ± 0.58	≤0.01*	0.02	0.02	0.55	0.81	0.99	1.00
BA	0.34 ± 0.16	0.31 ± 0.13	0.30 ± 0.14	-	-	0.31 ± 0.07	0.34 ± 0.14	0.54 ± 0.43	0.52 ± 0.31	≤0.01*	0.99	0.99	0.99	0.66	0.01	0.99
LA	0.55 ± 0.33	0.52 ± 0.23	0.56 ± 0.27	-	-	0.46 ± 0.20	0.54 ± 0.23	0.32 ± 0.23	0.36 ± 0.19	≤0.01*	0.99	1.00	0.69	0.91	0.01	0.99

*TbN is the number of trabeculae found in a selected region of bone. IQR: Interquartile range; CI: Central incisor; LI: Lateral incisor; C: Canine; DM1: Deciduous molar 1; DM2: Deciduous molar 2; PM1: Premolar 1; PM2: Premolar 2; M1: Molar 1; M2: Molar 2; AA: Apical average; BA: Buccal average; LA: Lingual average. *The significant values were less than 0.001 and were presented as p≤0.01. The p values of 0.003 and 0.002 in the lingual average of the deciduous dentition were presented as p ≤0.03 and p≤0.02, respectively.*

Table 12 Analysis of variance (ANOVA) indicating pairwise comparisons of TbSp for each dental crypt surface across dentition groups associated with the deciduous dentition, the mixed dentition, and the permanent dentition respectively.

	Median ± IQR										Pairwise comparison (p<0.05)					
	CI	**LI**	**C**	**DM1**	**DM2**	**PM1**	**PM2**	**M1**	**M2**	**Univariate p<0.05**	**CI vs. LI**	**LI vs. C**	**C vs D/PM 1**	**D/PM 1 vs. D/PM 2**	**D/PM 2 vs. M1**	**M1 vs. M2**
Deciduous (n = 28; 0 – 5 years)																
AA	0.84 ± 0.99	0.31 ± 0.18	0.45 ± 0.34	0.40 ± 0.35	0.54 ± 0.60	-	-	0.80 ± 0.91	-	≤0.01*	≤0.01*	0.91	0.99	0.99	0.87	-
BA	0.87 ± 1.40	0.98 ± 1.29	1.51 ± 0.89	1.32 ± 1.01	1.04 ± 1.29	-	-	0.77 ± 0.62	-	≤0.01	0.02	0.99	1.00	0.96	0.98	-
LA	0.61 ± 0.34	0.82 ± 0.57	0.59 ± 0.35	0.82 ± 0.51	0.81 ± 0.46	-	-	0.65 ± 0.42	-	≤0.02	0.02	≤0.04	0.09	1.00	0.86	-
Mixed (n = 9; 6 – 12 years)																
AA	0.47 ± 0.38	0.56 ± 0.72	0.49 ± 0.32	0.48 ± 0.28	0.78 ± 0.82	-	-	0.87 ± 0.69	-	≤0.14	0.95	0.59	1.00	0.98	1.00	-
BA	1.16 ± 0.92	1.57 ± 1.20	1.32 ± 1.15	1.20 ± 0.61	0.76 ± 0.53	-	-	0.97 ± 0.32	-	≤0.04	0.96	1.00	0.88	0.76	1.00	-
LA	0.57 ± 0.43	1.11 ± 0.75	0.74 ± 0.46	1.09 ± 1.23	1.31 ± 1.03	-	-	0.97 ± 0.55	-	≤0.14	0.56	0.97	0.58	1.00	1.00	-
Permanent (n = 42; 13 – 18 years)																
AA	0.25 ± 0.18	0.29 ± 0.21	0.31 ± 0.46	-	-	0.43 ± 0.36	0.43 ±0.30	0.42 ± 0.32	0.47 ± 0.27	≤0.75	0.59	1.00	1.00	1.00	1.00	1.00
BA	1.91 ± 1.23	1.78 ± 1.18	2.10 ± 1.11	-	-	2.01 ± 1.06	1.16 ± 1.03	0.77 ± 0.54	0.70 ± 0.71	≤0.01*	0.88	0.39	0.93	≤0.04	0.16	0.99
LA	0.79 ± 0.48	0.95 ± 0.67	0.88 ± 0.64	-	-	0.94 ± 0.59	0.87 ± 0.47	1.05 ± 0.71	1.03 ± 0.78	≤0.05	0.72	0.99	1.00	0.93	0.10	0.99

*TbSp is the trabecular spacing found in a selected region of bone. IQR: Interquartile range; CI: Central incisor; LI: Lateral incisor; C: Canine; DM1: Deciduous molar 1; DM2: Deciduous molar 2; PM1: Premolar 1; PM2: Premolar 2; M1: Molar 1; M2: Molar 2; AA: Apical average; BA: Buccal average; LA: Lingual average. *The significant values were less than 0.001 and were presented as p≤0.01.*

5 Discussion

The current study assessed the changes observed in the micro-architecture of the alveolar region of the postnatal and subadult human maxilla in relation to the development and eruption of the dentition. A key finding was the increased deposition of bone along the alveolar region leading to increases in the BV/TV and TbTh with dental development and eruption across the mixed dentition and the permanent dentition groups. The surface of bone available, presented as BS/BV and TbN both showed a decrease with the replacement of deciduous dentition with that of the permanent dentition. Lastly, the TbSp appeared to increase with age. The micro-architecture of the maxilla changed from a more porous to a more compact appearance as the teeth transitioned from unerupted deciduous to erupted deciduous and permanent dentition. The results in this study indicate that the alveolar bone of the maxilla adapts to accommodate the different stages of dentition. Thus, knowledge of these changes in the micro-architecture relative to the state of the dentition may be useful in the planning of dental procedures including orthodontic and endodontic treatment plans. In addition, this knowledge within the forensic setting is of value where juvenile age estimations may be required in the establishment of a biological profile.

In the deciduous dentition group, the maxillary alveolar bone was more porous in appearance demonstrated by a higher BS/BV ratio. The higher BS/BV may in turn be the reason for the higher TbN in this group, i.e., there is a higher TbN because there is more surface of the bone along the buccal, lingual, and apical regions of dental crypts in the deciduous dentition group. In contrast to the high BS/BV and TbN numbers observed, a reduced BV/TV ratio was observed within the deciduous dentition, which showed a decreased amount of bone despite an increase in bone surface. This is further confirmed by the lower TbTh observed within this group. The porous nature of the maxillary alveolar bone in the deciduous dentition group may also reflect the general growth of the maxilla (Scheuer and Black, 2000; Nanci, 2007).

The maxilla forms by intramembranous ossification in which bone develops directly within the connective tissue (Lee *et al*., 1992; Scheuer and Black, 2000). The first bone to be formed is called woven bone and consists of many islands of soft connective tissue. It is also highly vascular and characterized by osteons which are fewer in number and smaller in size. However, woven bone transitions into lamellar bone during the late stages of intrauterine life and the first years of postnatal life (Nanci, 2007). During this process of bone formation as well as during subsequent periods of bone growth, biomechanical demands emanating from the early functional environment i.e., suckling, are thought to be important contributors to the general remodeling of the maxilla as seen in the current study with the changes observed in the BS/BV and TbN ratios in the deciduous dentition group. It is also suggested that the remodeling of the alveolar bone of the jaws may be attributed to the dentition and the functional forces that are transferred from the teeth to the alveolar bone (Scheuer and Black, 2000; Huja *et al*., 2006; Huja and Beck, 2008).

The porous nature of the maxillary alveolar bone observed in the deciduous dentition group, i.e., higher BS/BV and TbN values and lower BV/TV and TbTh values in the current study may also be attributed to the state of dentition. The size of the deciduous dentition is relatively smaller when compared to the permanent dentition (Scheuer and Black, 2000; Schaefer *et al*., 2009), and therefore, less space is needed for the dentition in the deciduous dentition group. The smaller size of dentition relative to alveolar bone available may contribute to the higher BS/BV and values observed in the deciduous dentition. When teeth are still encased in the alveolar bone before eruption, there is little movement of the tooth germs and lesser biomechanical loads, and therefore less bone remodeling (Nanci, 2007; Lungová *et al.*, 2011). The lower levels of bone remodeling may contribute to the higher BS/BV and TbN and lower BV/TV and TbTh values observed. During the intraosseous phase of eruption, the dental follicle initiates the resorption of bone on the inferior aspect of the dental crypt and bone deposition on the superior aspect of the crypt (Nanci, 2007). As the tooth pierces through the gingiva, the dental follicle becomes the periodontal ligament, which is responsible for moving the tooth to its occlusal position and anchoring it to the dental crypt (Nanci, 2007; Wise and King, 2008). The emergence and subsequent eruption of the tooth crown from within the dental crypt marks a significant point when considering the relationship between the biomechanical loading and the associated functional environment of the oral cavity in general (Miller *et al.*, 2003; Wise and King, 2008).

The emergence and eruption of the deciduous dentition occurs in unison with functional demands of the masticatory system namely suckling and mastication (Miller *et al.*, 2003). During the early postnatal period (0 – 12 months), individuals are mainly suckling (Miller *et al.*, 2003), which means less biomechanical forces are exerted directly on the maxillary alveolar bone and hence the high BS/BV and TbN and low BV/TV and TbTh values in the individuals of the deciduous dentition group. Suckling the mother's breast includes the functioning of the lips, which are brought close to the gingival arch, widening it in the front. In contrast, bottle suckling is due to the tongue which pushes against the palate upwards (Dreyfus, 1925). Bruxism, which is a condition where individuals grind and clench teeth, is more prevalent and extensive in young children (Bodrumlu *et al.*, 2022). Bruxism may start as early as one year postnatally, but usually begins around four years of age (Saulue *et al.*, 2015). This condition can result in excessive wear and attrition of teeth, damage of the periodontal tissue, and movement of teeth (Saulue *et al.*, 2015; Bodrumlu *et al.*, 2022). All these forces acting on the deciduous dentition may influence the growth and the remodeling of the maxilla, for example, natural suckling forces will be transferred to the alveolar bone through the associated periodontal ligament which acts as a shock absorber and stimulates remodeling (Van Eijden, 2000).

The alveolar bone in the deciduous dentition appears to be less porous, demonstrated by increased BV/TV and TbN on the lingual and apical regions when compared to the buccal region. During early development, the bony crypts of the maxilla are wide open on the buccal side (Calonius *et al.*, 1970). This suggests that the lingual and the apical regions are more advanced in their development when compared to the buccal side of the dental crypts. The difference in the degree of development between the surfaces may further explain the micro-architectural differences of the three surfaces in the deciduous dentition group observed in the current study. The forces exerted by the tongue and the cheeks on the lingual and the buccal sides of the maxilla, respectively, are significantly different (Thüer *et al*., 1999). This difference was shown in a study where the pressure of the tongue and the cheek at rest and during chewing and swallowing were measured and the results showed that the pressures exerted on the lingual side are almost double the pressures exerted on the buccal side (Thüer *et al*., 1999). In this study, Thüer and colleagues (1999) aimed to measure the pressures acting on maxillary and mandibular teeth of 24 (12 male and 12 female) young adults aged 22 - 29 years using pressure transducers and electromyographic recording (Thüer *et al*., 1999). The micro-architecture on the apical region may be attributed to the fact that bone is deposited mainly on the apical region of the crypt during tooth eruption (Nanci, 2007; Wise and King, 2008). Compression forces exerted on the alveolar bone may also explain the more compact nature of trabeculae observed in the apical region (Yehuda *et al*., 2015).

The central incisors form and erupt before the lateral incisors in the maxilla (Kjaer 1988; Kjaer and Bagheri, 1999). However, the deciduous lateral incisor dental crypt is influenced by both the permanent central and lateral incisor successional teeth (AlQahtani *et al.,* 2010). This influence might explain the high ratio of BV/TV observed on the apical and buccal sides of lateral incisor when compared to the central incisor in the deciduous dentition group, i.e., there is more bone remodeling on the lateral incisor crypt when compared to the central incisor crypt. The same explanation may be used for the lower TbSp observed in all surfaces of the lateral incisor crypt when compared to central incisor crypt. In the deciduous dentition, the central incisor is closer to the buccal side and the lateral incisor is closer to the lingual side in the anteroposterior direction (Kawashima, 1976; Hiraide *et al*., 2008). It has been shown that the lingual side is more advanced in development when compared to the buccal side (Calonius *et al*., 1970). The pattern of growth of the buccal and lingual sides of the maxilla as well as the position of the lateral incisor in the deciduous dentition may explain the micro-architectural differences observed between the central and the lateral incisors.

The deciduous incisors erupt earlier when compared to the deciduous canines (AlQahtani *et al*., 2010; Esan and Schepartz, 2018). This pattern of eruption may contribute to the higher TbN and lower BV/TV ratio observed on the deciduous canine crypt when compared to the deciduous lateral incisor crypt. The deciduous and the permanent canine buds move labially during growth (Kjaer and Bagheri, 1999). This labial movement might be the reason for the maxillary canine prominence, which usually forms an elongated eminence that reaches to the lower border of the nasal aperture (Scheuer and Black, 2000). The labial movement may also be another reason for the difference in BV/TV between the lateral incisor crypt and the canine crypt observed within deciduous dentition.

As the dentition develops and erupts, the alveolar bone of the maxilla remodels to accommodate the developmental changes (Scheuer and Black, 2000). When comparing the deciduous dentition group and the mixed dentition groups, a change from a more porous to a less porous trabecular micro-architecture is observed. This change may be attributed to the higher functional and mechanical demands (Mavropoulos *et al*., 2004) that accompany growth and remodeling in the mixed dentition group when compared to the deciduous dentition, as well as the state of dentition (Scheuer and Black, 2000). The high TbN on the lingual side of the canine crypt in the deciduous dentition group when compared to that of the mixed dentition group may be attributed to higher remodeling rate in the mixed dentition group that is due to the replacement of deciduous dentition with permanent dentition. The slight increase in TbSp observed when comparing deciduous dentition group to mixed dentition group may be attributed to increased bone resorption that occurs during the shedding of deciduous dentition (Nanci, 2007). In other studies, there was no change observed in TbN (Kneissel *et al*., 1997; Parfitt *et al*., 2000; Rauch, 2007; Gabel *et al*., 2017), which is in contrast to the decrease in overall TbN with age in the current investigation between deciduous and mixed dentition groups. The difference in TbN in the current study may be attributed to changes in the alveolar bone from a woven bone type to a lamellar bone type which is more compact (Nanci, 2007).

In the mixed dentition group, a relatively higher BS/BV ratio was observed, i.e., there was still more alveolar bone surface observed and therefore high TbN. There was more alveolar bone deposition, which was presented as increased BV/TV and TbTh with little change in TbSp when compared to the deciduous dentition. The mixed dentition group is characterized by the shedding of deciduous dentition and replacement of this deciduous dentition by permanent dentition (Scheuer and Black, 2000; Schaefer *et al*., 2009). Thus, there is a need for space as the dentition increases in size and number. The maxillary alveolar bone undergoes intense remodeling to accommodate this increase in size and number of dentition (Scheuer and Black, 2000). The maxillary alveolar bone also accommodates this increase in size and number of dentition by elongation and growth of the maxilla in a mesial direction (Enlow and Bang, 1965). The incisive fissure also plays a role in accommodating the increased volume of dentition in the maxilla (Njio and Kjaer, 1993; Scheuer and Black, 2000). It is during this period of the shedding of dentition where the most dynamic changes in the shape and size of the alveolar bone occur (Lungová *et al.*, 2011). During the mixed dentition stage when teeth are shed, some teeth may be impacted. Teeth are considered impacted when they fail to erupt at the expected time and can no longer be expected to erupt (Hartman and Adlesic, 2021). These impacted teeth may affect the remodeling of the maxilla in the mixed dentition group. The maxillary sinus is closely related to the roots of the posterior maxillary dentition (Whyte and Boeddinghaus, 2019) and therefore, its development might have an effect on the growth of the maxilla in this region. The maxillary sinus growth occurs in three phases, with the first phase occurring during the first three years of postnatal life where the sinus extends lateral to the infraorbital canal. The second phase occurs between ages six and 12 years, which is the age range of the mixed dentition group in the current study. During this second phase, the maxillary sinus extends laterally to the maxillary zygomatic recess and inferiorly to the level of hard palate. Expansion of the sinus during the third phase is due to the pneumatization of the alveolus of the maxilla as the permanent premolar and molar teeth erupt (Scuderi *et al*., 1993; Lorkiewicz-Muszyńska *et al*., 2015; Whyte and Boeddinghaus, 2019). There is also an increased growth of the skeletal structures associated with the maxilla that occurs during this period. These structures include the maxillary tuberosity, zygomatic process, palatine process, the orbital surface, and the nasal region. These structures, as a collective, influence the growth of the maxilla in a complex variety of divergent directions, making it possible for the dental arch to remodel and lengthen (Enlow and Bang, 1965). Unlike the deciduous dentition group, the individuals in the mixed dentition group experience increased masticatory forces as they mainly bite and chew for successful intake of nutrients (Kaya *et al*., 2017).

When comparing the mixed dentition and the permanent dentition groups, the state of dentition as well as biomechanical forces may be the cause of the micro-architectural differences between the two dentition groups. During biting and mastication, any pressure from the dentition is transmitted directly to the trabecular bone (Moon *et al.*, 2004). In the mixed dentition, the deciduous dentition is shed and the roots are resorbed (Scheuer and Black, 2000; Nanci, 2007). This resorption of roots occurs on the lingual side of the deciduous dentition crypts. The subsequent shedding of the deciduous teeth may be attributed to the function of the dental follicle and the pressure of the developing permanent tooth, as well as the odontoclast action of the deciduous dentition (Nanci, 2007; Wise and King, 2008). This bone resorption during tooth shedding may be reason for the observed micro-architectural differences between the mixed and the permanent dentition groups. The number of teeth as well as tooth contact affects the biting force (Koc *et al*., 2010). The masticatory forces increase with age, and these changes are influenced by the loss of the deciduous dentition during the late mixed dentition phase of dental development (Barrera *et al*., 2011, Kaya *et al*., 2017). There are more teeth and contacts in the permanent dentition, and this may be one of the reasons for the higher BV/TV ratio on the apical region of the permanent central incisor crypt when compared to the deciduous incisor of the mixed dentition, as well as the lower BS/BV on the apical region of central and lateral incisors of the permanent dentition group when compared to those of the mixed dentition group.

The anterior maxillary dentoalveolar height (measured from the anterior nasal spine to the prosthion) is said to decrease with transition from mixed dentition to permanent dentition due to the loss of deciduous dentition (Laowansiri *et al.*, 2013). This decrease in dentoalveolar height might also contribute to the micro-architectural differences observed between the central incisors of the mixed dentition group and the permanent dentition group (Buschang *et al.*, 1983). The thickening of the trabeculae as dentition develops and erupts may also be caused by the general bone remodeling with a positive balance, i.e., there is more bone added than resorbed (Parfitt *et al.*, 2000; Rauch, 2007), and hence the higher TbTh in the permanent dentition group when compared to the mixed dentition group. It is also thought that the anterior teeth may drift in a distal direction to accommodate the growth of the bone in a mesial direction (Enlow and Bang, 1965). This drift may be another reason for the micro-architectural differences observed between the central and the lateral incisors of the mixed dentition group and the permanent dentition group, respectively.

The observed overall decrease in TbN as dentition transitions from mixed to permanent in the current study is in contrast to other studies in which no change was observed when using other skeletal elements during growth (Kneissel *et al.*, 1997; Parfitt *et al.*, 2000; Rauch, 2007; Gabel *et al.*, 2017). The decrease in TbN in this study may be attributed to the type of bone and the considerable difference in sample size of the groups compared. The permanent dentition group appeared to have a more mineralized alveolar ridge, which was mostly compact bone. The compact nature of the bone resulted in there being no TbTh, TbN, and TbSp to measure in some regions of interest. This observation may have affected the average of these parameters in the permanent dentition group and hence the difference in the micro-architecture of the permanent versus the mixed dentition groups. As the parameter values were averaged during comparison of dentition groups, the compact nature and therefore the lack of TbTh, TbN, and TbSp to measure had an effect on the overall values observed in the permanent dentition group.

The increase in TbSp in the permanent dentition group, which is in contrast to the decrease expected during growth (Rauch, 2007) was observed on the buccal and the lingual sides.

In the permanent dentition group, the bone is more matured, and this is presented as high BV/TV ratio and thicker trabeculae. The biomechanical forces associated with mastication and swallowing that are exerted on the maxillae with permanent dentition are the major cause of the observed compact micro-architecture of the alveolar bone (Bresin *et al*., 1999; Mavropoulos *et al*., 2004; Blok *et al*., 2013; Watson *et al*., 2018). The posterior dentition is said to experience the highest masticatory forces (Watson *et al*., 2018), and this may explain the higher BS/BV ratio found on the canine crypt when compared to the first premolar in the permanent dentition. The roots of the permanent first maxillary molar are said to be more curved than those of the premolars (Nyaga, 2010) and this may result in different occlusal forces between the two teeth (Watson *et al.*, 2018). The differences observed between the second premolar and the first molar in the permanent dentition may be due to these different occlusal forces which are higher on the first molar. Lateral incisors are relatively smaller and shorter when compared to the central incisors and canines (AlQahtani *et al.,* 2010; Esan and Schepartz, 2018) and this may explain the higher number of trabeculae on the lateral incisor crypt when compared to both the central incisor and canine crypts in the permanent dentition. The thickness of the buccal wall is said to increase in a mesiodistal direction (Jin *et al.*, 2012), and this may explain the higher BV/TV ratio on the buccal side of the second premolar when compared to the first premolar in the permanent dentition.

The fully matured state of the alveolar bone in the permanent dentition group is maintained by the tooth–periodontium–bone complex, also referred to as tooth–bone crosstalk (Fleischmannova *et al.,* 2010; Lungová *et al.*, 2011). The components of this complex function to disperse biomechanical loads that are exerted during mastication and maintain the homeostasis of the alveolar bone (Fleischmannova *et al.*, 2010; Naveh *et al*., 2012). The importance of this tooth-bone crosstalk and relationship between the alveolar bone and teeth is illustrated in the resorption of alveolar bone when teeth are lost (Scheuer and Black, 2000; Blair *et al.*, 2008). This resorption of the alveolar bone after the loss of teeth has been observed in older individuals (Ulm *et al.*, 1999, Scheuer and Black, 2000; Roberts and Hartsfield, 2004; Farina *et al.*, 2011; Kamigaki *et al.*, 2017).

While studies have assessed features of the maxilla and mandible trabeculation, the study subjects were adult individuals (Parfitt, 1988; Ulm *et al*., 1997; Lindh *et al*., 2004; Blok *et al*., 2013; Kim and Henkin, 2015; Monje *et al*., 2015). Thus, specific changes that occur during dental development and eruption have not been described. This limits the depth of inferences which can be made regarding the changes in the trabecular micro-architecture of the maxilla that take place during the complex stages of juvenile growth. In a study by Ulm *et al*. (1999), the trabecular micro-architecture of edentulous maxillae in individuals with a mean age of 72.5 years was described: BV/TV and TbTh decreased from the mesial region to the distal region, with the molar region presenting significantly lower BV/TV and TbTh when compared to the anterior region of incisors and canines. The observed differences between the mesial and distal regions was said to be attributed to molars being lost at earlier in most cases when compared to teeth in the mesial region (Ulm *et al*., 1999). The differences in the micro-architecture at different regions indicated site-specific changes that were also observed by other studies (Devlin *et al*., 1998; Lindh *et al*., 2004). Lindh *et al*. (2004) studied bone mineral density of the maxilla in edentulous individuals (aged between 51 and 79 years). The results showed that there were site-specific differences between the individuals. Bone mineral density was higher in the anterior region when compared to the posterior region (Lindh *et al*., 2004).

The success of dental implants is influenced by a number of factors such as bone mineral density, bone volume, and trabecular micro-architecture. While dental implants are not common in children with deciduous dentition, they may be needed in severe cases where loss or absence of teeth may result in loss of function and disturbances in the normal growth of the alveolar ridge (Agarwal *et al*., 2016). The current study provides information on the trabecular micro-architecture of the maxilla. This information may give some insights on the quality of alveolar bone at different stages of dental development, and hence predict the success of dental implants. Malocclusions are prevalent in both children and adults and are regarded as a third priority in oral health, after carries and periodontal disease (Ramson and Singh, 2021). These malocclusions may be corrected using orthodontic treatments such as dental braces. Dental braces function to move teeth to their normal functional position in the alveolar bone (Aggarwal *et al*., 2016). The trabeculation information from the current study may aid in planning the type and the duration of orthodontic treatment needed by juvenile patients.

6 Limitations

While this study provides useful information about the changes in micro-architecture of the maxilla in relation to dental development and eruption, there were some limitations. The sample was from skeletal remains, and therefore medical records were not available. This could lead to the inclusion of maxillae from individuals who presented with diseases that can affect the bone density and bone micro-architecture such as type 1 diabetes and cystic fibrosis (Fuusager *et al*., 2020; Putman *et al*., 2021). Although sex-specific changes were not assessed in the current study, it has been shown that permanent teeth erupt earlier in girls when compared to boys due the hormonal differences and early onset of maturation in girls (Peedikayil, 2011). While the study assessed the changes in trabecular bone, there was no separation of the cortical bone from the trabecular bone, which could have affected the readings of the trabecular parameters observed, as trabecular and cortical bones are different in structure. Trabecular bone has a web-like structure and compact bone is solid (Rüegsegger *et al*., 1991). The cross-sectional nature of the study may yield information about the dentition group differences but not necessarily changes in micro-architecture with dental development and eruption. The group with the smallest sample size was the mixed dentition group, and this is due to the limited material of this group in the collection of human skeletons used. In the future a longitudinal study, with the use of a low dose radiation modality such as cone beam CT (Monje *et al*., 2013; Liang *et al*., 2017), may be used assess the changes and differences in micro-architecture observed over the periods of dental development and eruption.

7 Conclusion

The micro-architecture of the maxillary alveolar changes during the different dentition stages were assessed. In the deciduous dentition group, the alveolar bone had a porous appearance, indicated by higher BS/BV and TbSp with lower BV/TV, TbTh and TbN. The mixed dentition group presented with a visible less porous alveolar bone, while the permanent dentition group presented with a more compact alveolar bone that was indicated by higher BV/TV and TbTh and lover BS/BV, TbN and TbSp. The changes observed between groups include a change from a more porous alveolar bone to a more compact alveolar bone as dentition stages advanced, represented by an increase in BV/TV, TbTh, TbSp and decrease in BS/BV and TbN. There is an increase in the deposition of bone as dentition advances, and this leads to the thickening of trabeculae. There are also site-specific changes in the micro-architecture of the maxilla, and these were observed in the comparison of crypts within groups. The patterns of micro-architectural changes observed in the maxilla between the dentition groups in this study reflect the general development and growth of the maxilla, state of dentition, the biomechanical forces, as well as the complex functional environment of the oral cavity. The results of the study may aid in the planning of orthodontic procedures by giving insights on the structure of the maxilla and the changes expected to take place at different stages.

Appendix A

UNIVERSITY OF THE WITWATERSRAND, JOHANNESBURG | FACULTY OF HEALTH SCIENCES | Anatomical Sciences

SCHOOL OF ANATOMICAL SCIENCES ETHICS WAIVER CLEARANCE LETTER

Faculty of Health Sciences
School of Anatomical Sciences
University of the Witwatersrand
Johannesburg

Re: In terms of Chapter 8, sections 62-64 of the National Health Act No 61 of 2003 donated bodies and their tissues may be used for, among other purposes, health, and research. Use of such Material is subject only to permission from the responsible person in the School of Anatomical Sciences – the Head or person designated by the Head of School.

Human Research Ethics Committee (Medical) Clearance Certificate:

W-CBP-220504-01

This letter serves to confirm that the Head of School, based in the School of Anatomical Sciences, Faculty of Health Sciences, has reviewed the research proposal entitled:

"Microarchitecture of the human postnatal maxilla in relation to tooth development and eruption"

by principal investigator: Mhlathi Xolisiwe

and supervisor/collaborators: Erin Hutchinson and Candice Small

and has granted approval for the ethics waiver to conduct the above-mentioned research study.

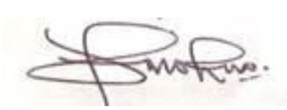

_____________________________ ___21-November-2022___

Professor Amadi O. Ihunwo
Head, School of Anatomical Sciences
Faculty of Health Sciences

Dated

School of Anatomical Sciences
7 York Rd, Parktown, 2193, South Africa, Private Bag 3, WITS 2050
Tel: +27 11 717 2405/2305 | www.wits.ac.za/anatomicalsciences/

UNIVERSITY OF THE WITWATERSRAND, JOHANNESBURG	HUMAN RESEARCH ETHICS COMMITTEE (MEDICAL)

Office of the Deputy Vice-Chancellor (Research & Innovation)

TO: Professor AO Ihunwo
School: Anatomical Sciences
Department:
Medical School
University

E-mail: Amadi.Ihunwo@wits.ac.za

CC: Supervisor: <>
and <HREC-Medical.ResearchOffice@wits.ac.za>

FROM: Mr Iain Burns
Human Research Ethics Committee (Medical)
Tel: 011 717 1252

E-mail: Iain.Burns@wits.ac.za

DATE: 04/05/2022

REF: *R14/49*

PROTOCOL NO: W-CBP-220504-01 (This is your ethics application study reference number. Please quote this reference number in all correspondence relating to this study)

PROJECT TITLE: *Research on cadaveric material*
Research conducted on donated bodies and their tissues
under sections 62-64 under the National Health Act No.61 of 2003
Formerly W-CJ-140604-1

Please find attached the Ethics Waiver Certificate for the above project. I hope it goes well and that an article in a recognized publication comes out of it. This will reflect well on your professional standing and contribute to the Government funding of the University.

MSWorks2000/Iain0007/ClearScanWaiver.wps

UNIVERSITY OF THE WITWATERSRAND, JOHANNESBURG	HUMAN RESEARCH ETHICS COMMITTEE (MEDICAL)

Office of the Deputy Vice-Chancellor (Research & Innovation)

04/05/2022

Ref: W-CBP-220504-01

TO WHOM IT MAY CONCERN

Waiver: This certifies that the following research does not require clearance from the Human Research Ethics Committee (Medical)

Investigator: Professor AO Ihunwo
Student No. (if appropriate):
Staff No. (if appropriate): 00500193

Supervisor:

School: Anatomical Sciences
Department:

Medical School
University

Project title: *Research on cadaveric material*
Research conducted on donated bodies and their tissues under sections 62-64 under the National Health Act No.61 of 2003
Formerly W-CJ-140604-1

Reason: Statutory waiver
No human participants will be involved in the study

Dr CB Penny
Chairperson: Human Research Ethics Committee (Medical)

Research Office Secretariat:
Third Floor, Phillip Tobias Building, corner of St Andrews and York Roads, Parktown, Johannesburg 2193
Postal address: Private Bag 3, Wits 2050
Tel Nos: +27 (0)11 717 1234/1252/2656/2700
Office E-mail: HREC-Medical.ResearchOffice@wits.ac.za
Website:
https://www.wits.ac.za/research/researcher-support/research-ethics/ethics-committees/

Appendix B

Lin's concordance correlation coefficient (Lin's CCC)

Lin's CCC was calculated using R studio by running the following code: CCC (x, y, ci = "z-transform", conf. level = 0.95, na.rm = FALSE).

x: first set of measurements

y: second set of measurements

ci: method used

na.rm: logical, indicating whether NA values should be stripped before the computation proceeds.

Table 13 Lin's concordance correlation coefficient for BV/TV.

Tooth	CI	LI	C	DM1	DM2	PM1	PM2	M1	M2
No. of teeth	9	9	9	5	5	4	4	8	4
No. of ROI	7	7	7	7	7	7	7	7	7
Intraobserver	0.94	0.92	0.90	0.87	0.92	0.97	0.90	0.93	0.93
Interobserver	0.82	0.82	0.90	0.70	0.90	0.93	0.90	0.96	0.88

BV/TV: bone volume to total volume ratio. ROI: region of interest. CI: central incisor. LI: lateral incisor. DM1&2: first and second deciduous molars. PM1&2: first and second premolars. M1&2: first and second molars.

Table 14 Lin's concordance correlation coefficient for BS/BV.

Tooth	CI	LI	C	DM1	DM2	PM1	PM2	M1	M2
No. of teeth	9	9	9	5	5	4	4	8	4
No. of ROI	7	7	7	7	7	7	7	7	7
Intraobserver	0.97	0.93	0.77	0.83	0.93	0.95	0.93	0.92	0.94
Interobserver	0.76	0.76	0.81	0.88	0.89	0.87	0.90	0.93	0.90

BS/BV: bone surface to bone volume ratio. ROI: region of interest. CI: central incisor. LI: lateral incisor. DM1&2: first and second deciduous molars. PM1&2: first and second premolars. M1&2: first and second molars.

Table 15 Lin's concordance correlation coefficient for trabecular thickness (TbTh).

Tooth	CI	LI	C	DM1	DM2	PM1	PM2	M1	M2
No. of teeth	9	9	9	5	5	4	4	8	4
No. of ROI	7	7	7	7	7	7	7	7	7
Intraobserver	0.92	0.82	0.68	0.92	0.95	0.70	0.50	0.52	0.91
Interobserver	0.66	0.51	0.94	0.84	0.90	0.46	0.80	0.78	0.82

TbTh: trabecular thickness. ROI: region of interest. CI: central incisor. LI: lateral incisor. DM1&2: first and second deciduous molars. PM1&2: first and second premolars. M1&2: first and second molars.

Table 16 Lin's concordance correlation coefficient for trabecular number (TbN).

Tooth	CI	LI	C	DM1	DM2	PM1	PM2	M1	M2
No. of teeth	9	9	9	5	5	4	4	8	4
No. of ROI	7	7	7	7	7	7	7	7	7
Intraobserver	0.82	0.90	0.83	0.92	0.91	0.92	0.81	0.90	0.94
Interobserver	0.62	0.70	0.75	0.80	0.87	0.74	0.81	0.92	0.82

TbN: trabecular number. ROI: region of interest. CI: central incisor. LI: lateral incisor. DM1&2: first and second deciduous molars. PM1&2: first and second premolars. M1&2: first and second molars.

Table 17 Lin's concordance correlation coefficient for trabecular spacing (TbSp).

Tooth	CI	LI	C	DM1	DM2	PM1	PM2	M1	M2
No. of teeth	9	9	9	5	5	4	4	8	4
No. of ROI	7	7	7	7	7	7	7	7	7
Intraobserver	0.82	0.91	0.95	0.93	0.94	0.97	0.86	0.92	0.90
Interobserver	0.68	0.87	0.87	0.76	0.86	0.94	0.86	0.91	0.80

TbSp: trabecular spacing. ROI: region of interest. CI: central incisor. LI: lateral incisor. DM1&2: first and second deciduous molars. PM1&2: first and second premolars. M1&2: first and second molars.

Technical error of measurement (TEM)

Table 18 Intraobserver error of 9 randomly selected individuals calculated using TEM.

	BV/TV	BS/BV	TbTh	TbN	TbSp
No. individuals	9	9	9	9	9
TEM	0.07	0.62	0.94	0.10	0.25
%TEM	14.01	18.31	87.31	16.23	23.22
R coefficient	0.93	0.93	0.67	0.90	0.93

TEM: technical error of measurement. BV/TV: bone volume to total volume ratio. BS/BV: bone surface to bone volume ratio. TbTh: trabecular thickness. TbN: trabecular number. TbSp: trabecular spacing.

Table 19 Interobserver error of 9 randomly selected individuals calculated using TEM.

	BV/TV	BS/BV	TbTh	TbN	TbSp
No. individuals	9	9	9	9	9
TEM	0.09	0.83	1.99	0.14	0.37
%TEM	18.77	24.70	161.36	21.92	34.74
R coefficient	0.87	0.87	0.71	0.81	0.83

TEM: technical error of measurement. BV/TV: bone volume to total volume ratio. BS/BV: bone surface to bone volume ratio. TbTh: trabecular thickness. TbN: trabecular number. TbSp: trabecular spacing.

Appendix C

For turnitin-2.docx

ORIGINALITY REPORT

15%	10%	12%	3%
SIMILARITY INDEX	INTERNET SOURCES	PUBLICATIONS	STUDENT PAPERS

PRIMARY SOURCES

1	wiredspace.wits.ac.za Internet Source	4%
2	N.V. Onwochei-bolum, B. Kramer, E.F. Hutchinson. "Taking shape: A geometric morphometric analysis of the immature human palate in relation to dental eruption and growth", Morphologie, 2024 Publication	1%
3	Erin F. Hutchinson, Mauro Farella, Jakobus Hoffman, Beverley Kramer. "Variations in bone density across the body of the immature human mandible", Journal of Anatomy, 2017 Publication	1%
4	www.researchgate.net Internet Source	1%
5	Craig Cunningham, Louise Scheuer, Sue Black. "The Skull", Elsevier BV, 2016 Publication	1%
6	L. J. PEREIRA. "Molar bite force and its correlation with signs of temporomandibular	1%

9 References

Agarwal, N., Kumar, D., Anand, A., and Bahetwar, S.K., 2016. Dental implants in children: A multidisciplinary perspective for long-term success. *National Journal of Maxillofacial Surgery*, 7(2), 122.

Aggarwal, I., Wadhawan, M., and Dhir, V., 2016. Myobraces: say no to traditional braces. *International Journal of Oral Care Research*, 4(1), 82-5.

Akintoye, S.O., 2018. The distinctive jaw and alveolar bone regeneration. *Oral Diseases*, 24(1–2), 49–51.

Allan, J.C., 1982. *Learning about statistics: a primer in simple statistical methods for students of the medical, biological, paramedical, social and behavioural sciences*. Macmillan.

AlQahtani, S.J., Hector, M.P., and Liversidge, H.M., 2010. Brief communication: The London atlas of human tooth development and eruption. *American Journal of Physical Anthropology*, 142(3), 481–490.

Bajić, V., Barbieri, C., Hübner, A., Güldemann, T., Naumann, C., Gerlach, L., Berthold, F., Nakagawa, H., Mpoloka, S.W., Roewer, L. and Purps, J., 2018. Genetic structure and sex-biased gene flow in the history of southern African populations. *American Journal of Physical Anthropology*, 167(3), 656-671.

Barrera, L.M., Buschang, P.H., Throckmorton, G.S. and Roldán, S.I., 2011. Mixed longitudinal evaluation of masticatory performance in children 6 to 17 years of age. *American Journal of Orthodontics and Dentofacial Orthopedics*, 139(5), 427-434.

Blair, H., Zaidi, M., Huang, C., Reviews, L.S.B., 2008. The developmental basis of skeletal cell differentiation and the molecular basis of major skeletal defects. *Biological Reviews*, 83(4), 401–415.

Blok, Y., Gravesteijn, F.A., Van Ruijven, L.J., and Koolstra, J.H., 2013. Micro-architecture and mineralization of the human alveolar bone obtained with microCT. *Archives of Oral Biology*, 58(6), 621–627.

Bodrumlu, E., Çakmak Özlü, F., Yılmaz, H. and Demiriz, L., 2022. Investigating the effect of bruxism on maxillary arch length and width in children using three-dimensional digital model analysis. *Progress in Orthodontics*, *23*, 1-7.

Bresin, A., Kiliaridis, S., and Strid, K.G., 1999. Effect of masticatory function on the internal bone structure in the mandible of the growing rat. *European Journal of Oral Sciences*, 107(1), 35–44.

Buschang, P.H., Baume, R.M., and Nass, G.G., 1983. A craniofacial growth maturity gradient for males and females between 4 and 16 years of age. *American Journal of Physical Anthropology*, 61(3), 373–381.

Buvinic, S., Balanta-Melo, J., Kupczik, K., Vásquez, W., Beato, C., and Toro-Ibacache, V., 2021. Muscle-bone crosstalk in the masticatory system: from biomechanical to molecular interactions. *Frontiers in Endocrinology*, 1197.

Calonius, P., Lunin, M., and Stout, F., 1970. Histologic criteria for age estimation of the developing human dentition. *Oral Surgery, Oral Medicine, Oral Pathology*, 29(6), 869–876.

Craddock, H.L. and Youngson, C.C., 2004. Eruptive tooth movement—the current state of knowledge. *British Dental Journal*, 197(7), 385-391.

Devlin, H., Horner, K., and Ledgerton, D., 1998. A comparison of maxillary and mandibular bone mineral densities. *The Journal of Prosthetic Dentistry*, 79(3), 323–327.

Dixon, A.D., 1997. Prenatal development of the facial skeleton. *In*: *Fundamentals of Craniofacial Growth*, 59–97.

Dreyfus, S., 1925. Influence of infant suckling methods on the development of the maxilla and on the production of adenoid characteristics. *International Journal of Orthodontia, Oral Surgery and Radiography*, 11(10), 902-906.

van Eijden, T.M.G.J., 2000. Biomechanics of the mandible. *Critical Reviews in Oral Biology and Medicine*, 11(1), 123–136.

Enlow, D.H. and Bang, S., 1965. Growth and remodeling of the human maxilla. *American Journal of Orthodontics*, 51(6), 446-464.

Esan, T.A. and Schepartz, L.A., 2018. The WITS Atlas: A Black Southern African dental atlas for permanent tooth formation and emergence. *American Journal of Physical Anthropology*, 166(1), 208–218.

Fan, Y., Li, Z., Loan, M., and Lv, C., 2011. Optimal principle of bone structure. *PLoS ONE*, 6(12), e28868.

Fanuscu, M.I. and Chang, T.L., 2004. Three-dimensional morphometric analysis of human cadaver bone: microstructural data from maxilla and mandible. *Clinical Oral Implants Research*, 15(2), 213–218.

Farina, R., Pramstraller, M., Franceschetti, G., Pramstraller, C., and Trombelli, L., 2011. Alveolar ridge dimensions in maxillary posterior sextants: a retrospective comparative study of dentate and edentulous sites using computerized tomography data. *Clinical Oral Implants Research*, 22(10), 1138–1144.

Fleischmannova, J., Matalova, E., Sharpe, P.T., Miseḱ, I., and Radlanski, R.J., 2010. Formation of the tooth-bone interface. *Journal of Dental Research*, 89(2), 108–115.

Fuusager, G., Milandt, N., Shanbhogue, V.V., Hermann, A.P., Schou, A.J., and Christesen, H.T., 2020. Lower estimated bone strength and impaired bone micro-architecture in children with type 1 diabetes. *BMJ Open Diabetes Research & Care*, 8(1) e001384.

Gabel, L., Macdonald, H.M., and McKay, H.A., 2017. Sex differences and growth-related adaptations in bone micro-architecture, geometry, density, and strength from childhood to early adulthood: a mixed longitudinal HR-pQCT study. *Journal of Bone and Mineral Research*, 32(2), 250–263.

Gahleitner, A., Watzek, G., and Imhof, H., 2003. Dental CT: imaging technique, anatomy and pathologic conditions of the jaws. *European Radiology*, 13, 366–376.

Hartman, B., and Adlesic, E.C., 2021. Evaluation and management of impacted teeth in the adolescent patient. *Dental Clinics*, 65(4), 805-814.

Hiraide, Y., Saka, H., Tamatsu, Y., Usami, A., Yanagisawa, N., and Ide, Y., 2008. Root resorption of maxillary primary incisors in relation to position of successive permanent incisors by Micro-CT. *Paediatric Dental Journal*, 18(1), 15–23.

Hovorakova, M., Lesot, H., Peterka, M., and Peterkova, R., 2018. Early development of the human dentition revisited. *Journal of Anatomy*, 233(2), 135–145.

Huja, S.S. and Beck, F.M., 2008. Bone remodeling in maxilla, mandible, and femur of young dogs. *The Anatomical Record,* 291(1), 1–5.

Huja, S.S., Fernandez, S.A., Hill, K.J., and Li, Y., 2006. Remodeling dynamics in the alveolar process in skeletally mature dogs. *The Anatomical Record,* 288(12), 1243–1249.

Hutchinson, E.F., Farella, M., Hoffman, J., and Kramer, B., 2017. Variations in bone density across the body of the immature human mandible. *Journal of Anatomy*, 230(5), 679–688.

Iscan, M.Y. and Steyn, M., 2013. *The human skeleton in forensic medicine*. Charles C Thomas Publisher.

Jin, S., Park, J., Kim, N., Park, S., Kim, K., Kim, Y., Kook, Y., and Ko, Y., 2012. The thickness of alveolar bone at the maxillary canine and premolar teeth in normal occlusion. *Journal of Periodontal & Implant Science*, 42(5), 173–178.

Kamigaki, Y., Sato, I., and Yosue, T., 2017. Histological and radiographic study of human edentulous and dentulous maxilla. *Anatomical Science International*, 92(4), 470–482.

Kardos, T.B., 1996. The mechanism of tooth eruption. *British Dental Journal*, 181(3), 91–95.

Kawashima, I.G.S., 1976. Studies on the changes of the crypt of the maxilla occurring as permanent teeth erupt. *Shikwa Gakuho*, 76, 1041–1098.

Kaya, M.S., Güçlü, B., Schimmel, M. and Akyüz, S.E.R.A.P., 2017. Two-colour chewing gum mixing ability test for evaluating masticatory performance in children with mixed dentition: validity and reliability study. *Journal of Oral Rehabilitation*, 44(11), 827-834.

Kim, J.E., Shin, J.M., Oh, S.O., Yi, W.J., Heo, M.S., Lee, S.S., Choi, S.C., and Huh, K.H., 2013. The three-dimensional microstructure of trabecular bone: Analysis of site-specific variation in the human jaw bone. *Imaging Science in Dentistry*, 43(4), 227–233.

Kim, S.T., Won, S.Y., Kim, S.H., Paik, D.J., Song, W.C., Koh, K.S., Kim, H.J., and Hu, K.S., 2011. Variations in the trabecular bone ratio of the maxilla according to sex, age, and region using micro-computed tomography in Koreans. *Journal of Craniofacial Surgery*, 22(2), 654–658.

Kim, Y.J. and Henkin, J., 2015. Micro-computed tomography assessment of human alveolar bone: bone density and three-dimensional micro-architecture. *Clinical Implant Dentistry and Related Research*, 17(2), 307–313.

Kjaer, I., 1988. Prenatal development of the maxillary primary incisors related to maturation of the surrounding bone and to postnatal eruption. *The Biological Mechanisms of Tooth Eruption and Root Resorption*, 233–236.

Kjaer, I. and Bagheri, A., 1999. Prenatal development of the alveolar bone of human deciduous incisors and canines. *Journal Dental of Research*, 78(2), 667–672.

Klintström, E., Smedby, K.B., Brismar, T.B., and Moreno, R., 2014. Trabecular bone histomorphometric measurements and contrast-to-noise ratio in CBCT. *Dentomaxillofacial Radiology*, 43(8) p.20140196.

Kneissel, M., Roschger, P., Steiner, W., Schamall, D., Kalchhauser, G., Boyde, A., and Teschler-Nicola, M., 1997. Cancellous bone structure in the growing and aging lumbar spine in a historic Nubian population. *Calcified Tissue International*, 61, 95-100.

Koc, D., Dogan, A. and Bek, B., 2010. Bite force and influential factors on bite force measurements: a literature review. *European Journal of Dentistry*, 4(02), 223-232.

Koch, J.C., 1917. The laws of bone architecture. *American Journal of Anatomy*, 21(2), 177–298.

Kopecka, D., Simunek, A., Bazda, T., Rota, M., Slezak, R., and Capek, L., 2012. Relationship between subsinus bone height and bone volume requirements for dental implants: a human radiographic study. *International Journal of Oral & Maxillofacial Implants*, 27(1), 48–54.

Langley, N.R., Jantz, L.M., McNulty, S., Maijanen, H., Ousley, S.D., and Jantz, R.L., 2018. Data for validation of osteometric methods in forensic anthropology. *Data in Brief*, 19, 21–28.

Laowansiri, U., Behrents, R.G., Araujo, E., Oliver, D.R., and Buschang, P.H., 2013. Maxillary growth and maturation during infancy and early childhood. *Angle Orthodontist*, 83(4), 563–571.

Lawrence, I., and Lin, K., 1989. A concordance correlation coefficient to evaluate reproducibility. *Biometrics*, 45, 255–268.

Lee, S.K., Kim, Y.S., Lim, C.Y., and Chi, J.G., 1992. Prenatal growth pattern of the human maxilla. *Cells Tissues Organs*, 145(1), 1–10.

Lewis, J.M., and Senn, D.R., 2010. Dental age estimation utilizing third molar development: A review of principles, methods, and population studies used in the United States. *Forensic Science International*, 201(1–2), 79–83.

Liang, X., Zhang, Z., Gu, J., Wang, Z., Vandenberghe, B., Jacobs, R., Yang, J., Ma, G., Ling, H., and Ma, X., 2017. Comparison of micro-CT and cone beam CT on the feasibility of assessing trabecular structures in mandibular condyle. *Dentomaxillofacial Radiology*, 46(5), p.20160435.

Lindh, C., Obrant, K., and Petersson, A., 2004. Maxillary bone mineral density and its relationship to the bone mineral density of the lumbar spine and hip. *Oral Surgery, Oral Medicine, Oral Pathology, Oral Radiology, and Endodontology*, 98(1), 102–109.

Liversidge, H., 2003. Dental development. *In*: *Patterns of Growth and Development in the Genus Homo*. 1st edition. Edited by Thompson J.L. Cambridge University Press, 37–73

Lorkiewicz-Muszyńska, D., Kociemba, W., Rewekant, A., Sroka, A., Jończyk-Potoczna, K., Patelska-Banaszewska, M. and Przystańska, A., 2015. Development of the maxillary sinus from birth to age 18. Postnatal growth pattern. *International Journal of Pediatric Otorhinolaryngology*, 79(9), 1393-1400.

Lungová, V., Radlanski, R.J., Tucker, A.S., Renz, H., Míšek, I., and Matalová, E., 2011. Tooth-bone morphogenesis during postnatal stages of mouse first molar development. *Journal of Anatomy*, 218(6), 699–716.

Maltha, J.C., 2014. Mechanisms of tooth eruption. *Netherlands Dental Journal*, 121(4), 209–214.

Mavropoulos, A., Kiliaridis, S., Bresin, A., and Ammann, P., 2004. Effect of different masticatory functional and mechanical demands on the structural adaptation of the mandibular alveolar bone in young growing rats. *Bone*, 35(1), 191–197.

Miller, J.L., Sonies, B.C., and Macedonia, C., 2003. Emergence of oropharyngeal, laryngeal and swallowing activity in the developing fetal upper aerodigestive tract: an ultrasound evaluation. *Early Human Development*, 71(1), 61–87.

Monje, A., González-García, R., Monje, F., Chan, H.-L., Galindo-Moreno, P., Suarez, F., and Wang, H.-L., 2015. Micro-architectural pattern of pristine maxillary bone. *The International Journal of Oral & Maxillofacial Implants*, 30(1), 125–132.

Monje, A., Monje, F., Ul Gonz Alez-Garc, R., Galindo, P., Francisco, -Moreno, Wang, R.-S.H.-L., Wang, H.-L., Ul Gonz Alez-Garc Ia, R., Galindo-Moreno, P., Rodriguez-Salvanes, F., and Mir, C.J., 2013. Comparison between microcomputed tomography and cone-beam computed tomography radiologic bone to assess atrophic posterior maxilla density and macroarchitecture. *Clinical Oral Implants Research*, 25(6), 723–728.

Moon, H.S., Won, Y.Y., Kim, K.D., Ruprecht, A., Kim, H.J., Kook, H.K., and Chung, M.K., 2004. The three-dimensional microstructure of the trabecular bone in the mandible. *Surgical and Radiologic Anatomy*, 26(6), 466–473.

Nanci, A., 2007. *Ten Cate's oral histology: development, structure, and function*. 7th ed. Mosby Elsevier, St. Louis, United States.

Narnbiar, P., 1995. Age estimation using third molar development. *Malaysian Journal of Pathology*, 17(1), 31–34.

Naveh, G.R., Chattah, N.L.T., Zaslansky, P., Shahar, R., and Weiner, S., 2012. Tooth–PDL–bone complex: Response to compressive loads encountered during mastication–A review. *Archives of Oral Biology*, 57(12), 1575-1584.

Njio, B. and Kjaer, I., 1993. The development and morphology of the incisive fissure and the transverse palatine suture in the human fetal palate. *Journal of Craniofacial Genetics and Developmental Biology*, 13(1), 24–34.

Nyaga, J., 2010. External and internal root morphology of the first permanent molars in a Kenyan population (Doctoral dissertation, University of Nairobi).

Parfitt, A.M., 1988. Bone histomorphometry: proposed system for standardization of nomenclature, symbols, and units. *Calcified Tissue International*, 42(5), 284–286.

Parfitt, A.M., Travers, R., Rauch, F., and Glorieux, F.H., 2000. Structural and cellular changes during bone growth in healthy children. *Bone*, 27(4), 487-494.

Park, H.S., Lee, Y.J., Jeong, S.H., and Kwon, T.G., 2008. Density of the alveolar and basal bones of the maxilla and the mandible. *American Journal of Orthodontics and Dentofacial Orthopedics*, 133(1), 30–37.

Peedikayil, F.C., 2011. Delayed tooth eruption. *Journal of Dentistry*, 1(4), 81-86.

Petersen, D.C., Libiger, O., Tindall, E.A., Hardie, R.A., Hannick, L.I., Glashoff, R.H., Mukerji, M., Fernandez, P., Haacke, W., Schork, N.J., and Hayes, V.M., 2013. Complex patterns of genomic admixture within Southern Africa. *PLoS Genetics*, 9(3), e1003309.

Peterson, J., Wang, Q., and Dechow, P.C., 2006. Material properties of the dentate maxilla. *The Anatomical Record,* 288A(9), 962–972.

Pramstraller, M., Farina, R., Franceschetti, G., Pramstraller, C., and Trombelli, L., 2011. Ridge dimensions of the edentulous posterior maxilla: a retrospective analysis of a cohort of 127 patients using computerized tomography data. *Clinical Oral Implants Research*, 22(1), 54–61.

Putman, M.S., Greenblatt, L.B., Bruce, M., Joseph, T., Lee, H., Sawicki, G., Uluer, A., Sicilian, L., Neuringer, I., Gordon, C.M., Bouxsein, M.L., and Finkelstein, J.S., 2021. The effects of ivacaftor on bone density and micro-architecture in children and adults with cystic fibrosis. *The Journal of Clinical Endocrinology and Metabolism*, 106(3), e1248.

Ramson, K. and Singh, S., 2021. Orthodontic status and treatment need of 13 to 15 year-old children in Kwa-Zulu Natal South Africa: An epidemiology study using the Dental Aesthetic Index (DAI). *South African Dental Journal*, 76(7), 414-421.

Rauch, F., 2007. Bone accrual in children: adding substance to surfaces. *Pediatrics*, 119(2), 137–140.

Roberts, W.E., and Hartsfield, J.K., 2004. Bone development and function: genetic and environmental mechanisms. *Seminars in Orthodontics*, 10(2), 100–122.

Rüegsegger, P., Durand, E.P., and Dambacher, M.A., 1991. Differential effects of aging and disease on trabecular and compact bone density of the radius. *Bone*, 12(2), 99–105.

Sánchez, M.J., Vicente, A., and Bravo, L.A., 2009. Third molar agenesis and craniofacial morphology. *Angle Orthodontist*, 79(3), 473-478.

Saulue, P., Carra, M.C., Laluque, J.F., and d'Incau, E., 2015. Understanding bruxism in children and adolescents. *International Orthodontics*, 13(4), 489-506.

Schaefer, M., Black, S., and Scheuer, L., 2009. *Juvenile osteology: a laboratory and field manual*, 1st edition, Elsevier Academic Press, Burlington, United States.

Scheuer, L., and Black, S.M., 2000. *Developmental juvenile osteology*, 1st edition, Elsevier Academic Press, London, England.

Scuderi, A.J., Harnsberger, H.R., and Boyer, R.S., 1993. Pneumatization of the paranasal sinuses: normal features of importance to the accurate interpretation of CT scans and MR images. *AJR. American Journal of Roentgenology*, 160(5), 1101-1104.

Sisman, Y., Uysal, T., Yagmur, F., and Ramoglu, S.I., 2007. Third-molar development in relation to chronologic age in Turkish children and young adults. *The Angle Orthodontist*, 77(6), 1040–1045.

Solari, A.A. and Abramovitch, K., 2002. The accuracy and precision of third molar development as an indicator of chronological age in Hispanics. *Journal of Forensic Sciences*, 47(3), 531–535.

Soriano, R.M. and Das, J.M., 2022. Anatomy, Head and Neck, Maxilla. In *StatPearls [Internet]*. StatPearls Publishing.

South African National Health Act 61 of 2003 https://www.gov.za/documents/acts/national-health-act-61-2003-23-jul-2004#:~:text=The%20National%20Health%20Act%2061,regard%20to%20health%20services%3B%20and (Accessed: 29 November 2023).

Stauber, M. and Müller, R., 2008. Micro-computed tomography: A method for the non-destructive evaluation of the three-dimensional structure of biological specimens. *Methods in Molecular Biology*, 455, 273–292.

Thüer, U., Sieber, R., and Ingervall, B., 1999. Cheek and tongue pressures in the molar areas and the atmospheric pressure in the palatal vault in young adults. *European Journal of Orthodontics*, 21(3), 299–309.

Trevizan, M., Nelson Filho, P., Franzolin, S.D.O.B. and Consolaro, A., 2018. Premaxilla: up to which age it remains separated from the maxilla by a suture, how often it occurs in children and adults, and possible clinical and therapeutic implications: Study of 1,138 human skulls. *Dental Press Journal of Orthodontics*, 23,16-29.

Ulm, C.W., Kneissel, M., Schedle, A., Solar, P., Matejka, M., Schneider, B., and Donath, K., 1999. Characteristic features of trabecular bone in edentulous maxillae. *Clinical Oral Implants Research*, 10(6), 459–467.

Ulm, C.W., Kneissel, M., Hahn, M., Solar, P., Matejka, M., and Donath, K., 1997. Characteristics of the cancellous bone of edentulous mandibles. *Clinical Oral Implants Research*, 8(2), 125–130.

Watson, P.J., Fitton, L.C., Meloro, C., Fagan, M.J., and Gröning, F., 2018. Mechanical adaptation of trabecular bone morphology in the mammalian mandible. *Scientific Reports*, 8(1), 1–12.

Whyte, A., and Boeddinghaus, R., 2019. The maxillary sinus: physiology, development and imaging anatomy. *Dentomaxillofacial Radiology*, 48(8), p.20190205.

Wise, G.E., and King, G.K., 2008. Mechanisms of tooth eruption and orthodontic tooth movement. *Journal of Dental Research*, 87(5), 414–434.

Wolff, J., 1986, *The Law of Bone Remodelling*, 1st edition, Springer Berlin, Heidelberg, Germany.

Yehuda, A.B, Singer, C., and Katz, J., 2015. About gravity and occlusal forces in the jaws: Review. *World Journal of Stomatology*, 4(4), 126–128.